

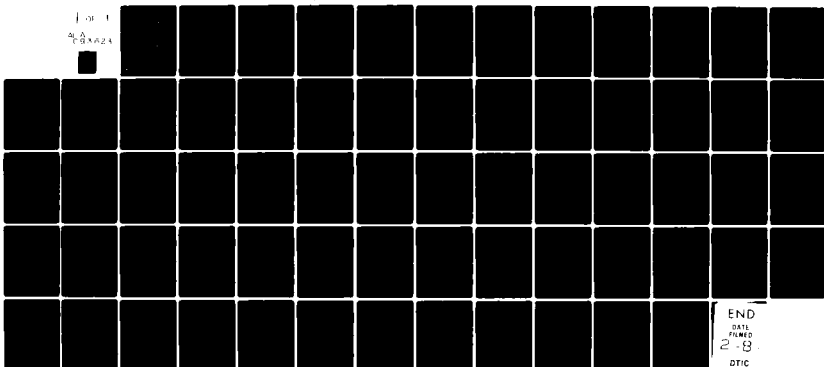
AD-A093 623

STANFORD UNIV CALIF STANFORD ELECTRONICS LABS
PREPARATION AND PROPERTIES OF AL(X)6A(1-4)AS:CR SINGLE CRYSTALS--ETC(U)
SEP 80 G L PEARSON

F/6 20/12
N00014-78-C-0297
NL

UNCLASSIFIED

Form 1
46-A
GSA GEN 24



END
DATE
FILED
2-18
DTIC

AD A093623

(6) PREPARATION AND PROPERTIES OF $\text{Al}_x\text{Ga}_{1-x}\text{As:Cr}$
SINGLE CRYSTALS.

(12)

(11), September 1980

LEVEL II

(?) Final Report. 1 Oct 77-31 Aug 81

Covering the Period 1 October 1977

through 31 August 1980

(12) 66



Prepared Under

Office of Naval Research

Contract Number N00014-78-C-0297

(15)

(10) Gerald L. Pearson

Solid State Electronics Laboratory
Stanford Electronics Laboratories
Stanford University, Stanford, California 94305

DATA	STATEMENT A
Approved:	RTIC release;
Approved:	Unlimited

332400 DM

80 10 3 22

DMC FILE COPY

TABLE OF CONTENTS

<u>Section</u>		<u>Page</u>
	Foreword	1
I	Summary	2
II	Accomplishments During the Period 1 Oct 1977 - 31 Aug 1980	4
III	References	10
Appendix A	The Cr ²⁺ Level in Al _x Ga _{1-x} As:Cr Single Crystals, K. Kocot and G. L. Pearson, Bull. Am. Phys. Soc. <u>23</u> , 17 (1978).	
Appendix B	Experimental Verification of Cr ²⁺ Models of Photoluminescent Transitions in GaAs:Cr and Al _x Ga _{1-x} As:Cr Single Crystals, K. Kocot and G. L. Pearson, Solid State Communications <u>25</u> , 113 (1978).	
Appendix C	Properties of Cr Deep Levels in Al _x Ga _{1-x} As:Cr, K. Kocot, R. A. Rao, and G. L. Pearson, Phys. Rev. B <u>19</u> , 2059 (1979).	
Appendix D	Quarterly Report - July 1979	
Appendix E	Quarterly Report - October 1979	
Appendix F	Quarterly Report - January 1980	
Appendix G	Quarterly Report - June 1980	

Accession For	
NTIS GRA&I <input checked="" type="checkbox"/>	
DTIC TAB <input type="checkbox"/>	
Unannounced <input type="checkbox"/>	
Justification <i>per Letter on file</i>	
By _____	
Distribution/ _____	
Available Codes _____	
Title Ref or _____	
Dist _____	
A	_____
_____	_____
_____	_____

FOREWORD

The Stanford Electronics Laboratories has conducted research on "Preparation and Properties of $\text{Al}_x\text{Ga}_{1-x}\text{As:Cr}$ Single Crystals" from 1 October 1977 through 31 August 1980 under ONR Contract N00014-78-C-0297. Funding did not actually begin until February 1978. The work was carried out under a one year contract followed by a five month no cost extension. The contract was then renewed for a period of one year and this was followed by a six month no cost extension. The contract, which was funded in the total amount of \$97,802, terminated on 31 August 1980. The Scientific Officer during this entire period was Dr. Howard Lessoff of the Naval Research Laboratory, Code 5220. Technical assistance from Dr. Harry Wieder and his group at the Naval Ocean Systems Center, Code 922, is gratefully acknowledged.

The personnel at the Stanford Research Laboratories included:

Professor Gerald L. Pearson	-- Principal Investigator
Mr. C. Kocot, Staff	-- 1 Oct 1977 - 1 Sept 1978
Dr. R. Rao, Staff	-- 1 Oct 1977 - 1 Sept 1978
Mr. M. Landstrass, Staff	-- 1 Oct 1978 - 31 Aug 1980

I. SUMMARY

This research program is divided into the following four related topics: (1) Growth of $\text{Al}_x\text{Ga}_{1-x}\text{As:Cr}$ thin semi-insulating (SI) layers by liquid phase epitaxial (LPE) techniques, (2) Properties of Cr deep levels in $\text{Al}_x\text{Ga}_{1-x}\text{As:Cr}$ single crystals (3) Investigation of the interface properties of (SI) $\text{Al}_x\text{Ga}_{1-x}\text{As:Cr-(n)GaAs}$ heterojunctions and (4) Construction and properties of Au-(SI) $\text{Al}_x\text{Ga}_{1-x}\text{As:Cr-(n)GaAs-(SI)GaAs:Cr}$ MIS field effect transistor structures.

Methods have been developed for reproducibly growing high quality Cr doped single crystal layers having selected values of x between 0.0 and 0.9 with specified thicknesses between 300 Å and several μm . Resistivities up to 10^{11} ohm-cm have been obtained.

The peak energy of the photoluminescent band due to Cr^{2+} was observed at 0.8 eV in Cr doped crystals regardless of Al composition between $0 \leq x \leq 0.74$ when measured at 77 K. The optical ionization energies of Cr^{2+} with respects to the conduction and valence bands were determined from photocapacitance measurements in crystals having the same range of x. Photoconductivity measurements were carried out which establish the degeneracy range of the $\text{Cr}^{2+}(5E)$ excited level with respect to the conduction band as x is varied from 0.0 to 0.6. Alternate models of photoluminescent intrairmpurity transitions from Cr levels in n- and p-type crystals were analyzed.

I-V, C-V and G-V measurements were made on Au/Pt-(SI) $\text{Al}_{0.5}\text{Ga}_{0.5}\text{As:Cr-(n)GaAs}$ diodes with temperature, frequency and illumination as the independent variables. The results were analyzed to determine the

current-transport mechanisms as well as to obtain information on the localized states and electron potential at the (SI)AlGaAs-GaAs interface.

Two different insulated gate field-effect transistor structures were designed which consist of (1) a self aligned p-channel device formed by Zn diffusion and (2) an n-channel transistor formed by e-beam lithography and sulfur ion implants. Electrical measurements on the former established that a p-channel was formed and quantitative values of its properties were obtained. The latter is still under development.

II. ACCOMPLISHMENTS DURING THE PERIOD

1 OCT 1977 - 31 AUG 1980

The Stanford Electronics Laboratories has been conducting research on the preparation and properties of $\text{Al}_x\text{Ga}_{1-x}\text{As:Cr}$ single crystals under ONR Contract No. 00014-78-C-0297 since 1 October 1977. Emphasis was placed on determining the energy states associated with Cr^{2+} together with the various transitions involved. Preparation of thin semi-insulating $\text{Al}_x\text{Ga}_{1-x}\text{As:Cr-GaAs}$ heterojunctions by LPE techniques and investigation of their use in high frequency MIS field effect transistor structures were initiated during the latter part of the contract.

The chief accomplishments of these studies were:

1. A horizontal carbon boat sidebar LPE system was used to grow $\text{Al}_x\text{Ga}_{1-x}\text{As:Cr}$ and $\text{Al}_x\text{Ga}_{1-x}\text{As:Fe}$ single crystal layers of prescribed Cr and Fe content. The Al fraction was varied to obtain values of x between 0.0 and 0.6.
2. Photoluminescence spectra from Cr doped crystals having a range of Al composition x from 0.0 to 0.6 were recorded while the sample was maintained at 77°K. The excitation source was an Ar ion laser capable of producing 4 W of cw radiation. The composition x of each crystal was determined from the energy of the band-to-band radiation. The spectrum arising from transitions due to Cr^{2+} ions in each crystal was recorded. Whereas the band gap increased with x , the peak energy of the Cr^{2+} photoluminescent band remained constant at 0.78 eV for all values of x [1]. This result corroborates the excited state to ground state transition model proposed by Koschel et al. [2].

3. Samples of $\text{Al}_x\text{Ga}_{1-x}\text{As:Cr}$ and $\text{Al}_x\text{Ga}_{1-x}\text{As:Fe}$ single crystals were sent to Dr. B. D. McCombe at NRL to investigate the zero-phonon line in these crystals as a function of x at 4.2 K. Although the normal zero phonon line at 840 meV was observed in the GaAs:Cr crystal ($x = 0$), it was absent in all mixed crystals within the range $x = 0.13 - 0.60$. The phonon replica peaked at 0.77 eV in all Al bearing crystals as compared with 0.825 when $x = 0$. The intensity of the 0.77 eV band peaked sharply at $x = 0.3$ and disappeared as x approached either 0.0 or 0.60.

A strong zero-phonon line at 0.37 eV, characteristic of Fe, was observed in GaAs:Fe ($x = 0$). This line also appeared at the same energy in a $\text{Al}_{0.33}\text{Ga}_{0.67}\text{As:Fe}$ sample, although the intensity was greatly reduced.

4. Photocapacitance was employed to measure the optical ionization energies of Cr^{2+} with respect to the conduction and valence bands in $\text{Al}_x\text{Ga}_{1-x}\text{As:Cr}$ crystals as a function of Al composition x . It was shown that the sum of the optical ionization energies of Cr^{2+} exceeds the direct energy gap by an amount ΔE , the magnitude of which decreases with increase in x . An explanation of this result was given in terms of the conduction band structure and Stokes' shift [3].
5. Photoconductivity measurements were carried out which establish the degeneracy range of the $\text{Cr}^{2+}(5E)$ excited level with respect to the conduction band as x is varied from 0.0 to 0.60. It was shown that the $5E$ excited state lies within the

conduction band for values of x below 0.23 and within the band gap when x is greater than 0.38 [3]. Further measurements are required to establish the exact crossover point.

6. Multilayer structures were grown by LPE techniques. The general configuration of these single crystal heterojunction samples, which were deposited on the 100 surface of either semi-insulating GaAs:Cr or (n^+)GaAs:Te substrates, was $(SI)Al_{0.5}Ga_{0.5}As:Cr-GaAs$. The GaAs active layers were 4-10 μm in thickness. Undoped layers were n-type with a carrier concentration of $\approx 1 \times 10^{15} \text{ cm}^{-3}$. Others were made p-type by adding sufficient Ge to bring the carrier concentration to $\approx 1 \times 10^{16} \text{ cm}^{-3}$. The semi-insulating $Al_{0.5}Ga_{0.5}As:Cr$ layers were grown to a thickness of $\approx 8000 \text{ \AA}$. They were prepared by adding 0.5 atomic % Cr to the melt. Close compensation of shallow donors and acceptors in the melt was achieved by baking out at 474°C for 40 to 100 hr in flowing H_2 just prior to growth. The resistivity of the SI layer obtained by this procedure was $\approx 1 \times 10^{11} \text{ ohm cm}$.
7. MIS diodes were fabricated by applying ohmic Au/Ge contacts to the substrates (or the GaAs active layers) and $1 \times 10^{-3} \text{ cm}^{-3}$ Cr/Pt dots to the $Al_{0.5}Ga_{0.5}As:Cr$ semi-insulating layers. The conduction current was measured as a function of voltage, temperature, frequency and illumination. It was found that the current through the $Al_{0.5}Ga_{0.5}As:Cr$ layer was controlled by injection from the Cr/Pt dot and the GaAs active layer. Under low injection conditions the semi-insulating layer was ohmic whereas Fowler-Nordheim type tunneling dominated at

high injection levels. Current in the device saturated at very high injection in the inversion polarity due to the limited supply of thermally generated minority carriers.

This was demonstrated by the use of light to control the current level in the saturated region. See references in Appendix E.

8. C-V and G-V measurements were made on $\text{Al}_{0.5}\text{Ga}_{0.5}\text{As:Cr-(n)GaAs}$ capacitors as a function of frequency and temperature in order to determine the distribution of localized states and the electron potential in the GaAs layer at the heterojunction interface. Capacitors with 8000 Å $\text{Al}_{0.5}\text{Ga}_{0.5}\text{As:Cr}$ layers showed that the GaAs surface was always accumulated while thin layers of 500 Å produced depleted surfaces. The zero bias potential could be consistently described as due to a metal- $\text{Al}_{0.5}\text{Ga}_{0.5}\text{As:Cr}$ interaction similar to the effect of the metal work function in Si-SiO₂ capacitors. Measurements on 8000 Å structures with frequency as the independent variable always showed a large frequency dispersion in both capacitance and conductance. This was shown to be due to trapping effects in the $\text{Al}_{0.5}\text{Ga}_{0.5}\text{As:Cr}$ layer where modulation of the thermal emission of carriers from the traps increased with decreasing frequency. This effect was also observed in $\text{Al}_{0.5}\text{Ga}_{0.5}\text{As:O}$ layers prepared by molecular beam epitaxy as measured on samples furnished by H. C. Casey et al. [4]. Another form of frequency dispersion was observed which was due to tunnel injection of carriers into the semi-insulating layer. This mechanism was established from its lack of temperature sensitivity.

9. Two inversion channel transistor structures were designed to measure surface potential and the time dependence of interface states. A self aligned p-channel device was fabricated which used a Cr/Pt metal gate to define the channel etch as well as the Zn diffused source and drain contacts to the n-type active layer. Two terminal measurements which were made with the gate shorted to the drain and the source grounded. These indicated that a p-channel was formed. The I-V characteristics were exponential below ≈ 3 V and thereafter gave a straight line on an \sqrt{I} vs V plot. Three terminal measurements were performed at gate voltages between 0 and 17 V. A plot of channel conductance versus gate voltage yielded a straight line giving a hole mobility of $300 \text{ cm}^2/\text{V}\cdot\text{sec}$ and a turn on voltage of 4 V.

An n-channel transistor is currently in the processing stage. This device employs e-beam lithography to define a channel width of $\approx 3 \mu\text{m}$ and sulphur ion implants into an (SI) GaAs:Cr substrate for the source and drain contacts. This device which is a normally off n-channel inversion mode MISFET has the advantage that the channel is semi-insulating when off, in contrast to being p-type, which assures low capacitance and sidesteps the problems of a low barrier height for injection of holes into the $\text{Al}_{0.5}\text{Ga}_{0.5}\text{As:Cr}$ layer. The fact that the channel length is shorter than the diffusion length of electrons should insure rapid response of n-channel formation.

10. The combined results of our measurements indicate Fermi level pinning does not exist at the (SI)Al_{0.5}Ga_{0.5}As:Cr-GaAs interface so that the GaAs surface potential can respond to DC bias. This is supported by (1) lack of any unaccounted for shift in flat band voltage; (2) C-V characteristics which indicate an accumulated surface at zero bias potential; and (3) MIS transistor measurements which demonstrate a hole inversion layer. This shows that in such a structure, just as in the Si/SiO₂ system, a DC bias can modulate the surface potential from accumulation to inversion. Unlike the Si/SiO₂ structure, however, an external supply of carriers is needed for quasi-equilibrium conditions to be observed due to the low thermal generation rate and a low barrier for hole injection into the insulating layer.

III. REFERENCES

1. K. Kocot and G. L. Pearson, Solid State Comm. 25, 113 (1978).
2. W. H. Koschel, S. G. Bishop and B. D. McCombe, Solid State Comm. 19, 521 (1976).
3. K. Kocot, R. A. Rao, and G. L. Pearson, Phys. Rev. B 19, 2059 (1979).
4. H. C. Casey, Jr., A. Y. Cho, D. V. Lang and E. C. Nicollian, J. Vac. Sci. Technol. 15, 1408 (1978).

APPENDIX A

San Francisco Meeting of the American Physical Society
January 23-26, 1978

AG 6 The Cr²⁺ Level in Al_xGa_{1-x}As Single Crystals.
K. KOCOT and G. L. PEARSON, Stanford U.-> LPE layers of
Al_xGa_{1-x}As:Cr single crystals were grown. The photoluminescence band due to Cr²⁺ was observed over the range
0 < x < 0.74, in both n and p-type crystals when measured at 77K. The peak energy of the Cr²⁺ band was constant at
0.8 eV for all values of x. Preliminary spectra which
reveal the characteristic zero phonon line were obtained
at 4.2K for x = 0.23. The position of the Cr²⁺ ground
level with respect to the bottom of the conduction band
was determined from photocapacitance measurements on n-
type Al_xGa_{1-x}As:Cr. It increased linearly from 0.85 to 1.1
eV as x changed from 0 to 0.47, when measured at 295K.
These values were about 0.08 eV higher when measured at
77K. Photocapacitance measurements performed on p-type
Al_xGa_{1-x}As:Cr located the Cr²⁺ level with respect to the
top of the valence band. The ionization energy of the
Cr²⁺ level with respect to the valence band increased li-
nearly from 0.81 eV to 0.91 eV as x changed from 0 to 0.4,
when measured at 295K. Stoke's shift has been calculated.
Our results favor the photoluminescence model proposed by
Kuschel et al rather than that of Stocker et al and en-
abled us to establish a more sophisticated model.

Bulletin of the American Physical Society 23, 17 (1978)

APPENDIX B

**EXPERIMENTAL VERIFICATION OF Cr²⁺ MODELS OF PHOTOLUMINESCENT TRANSITIONS IN
GaAs:Cr AND Al_xGa_{1-x}As:Cr SINGLE CRYSTALS**

K. Kocot* and G.L. Pearson

Stanford Electronics Laboratories, Stanford University, Stanford, CA 94305, U.S.A.

(Received 8 August 1977 by H. Suhl)

LPE layers of Al_xGa_{1-x}As:Cr:Sn single crystals were grown and the photoluminescence band due to Cr²⁺ was observed over the range 0 < x < 0.42 when measured at 77 K. Preliminary spectra which reveal the characteristic zero phonon line were obtained at 4.2 K for x = 0.23. The experimental results support the model in which the 0.84 eV photoluminescence band in GaAs:Cr is attributed to intraimpurity transitions at Cr²⁺.

IN RECENT YEARS, interest has increased in GaAs:Cr not only because of its use as a semi-insulating substrate for epitaxial crystal growth, but also because of its potential applications in numerous electronic devices such as field effect transistors and photodetectors. Despite a large number of investigations, the detailed nature of defects due to Cr in GaAs has not been firmly established. The typical photoluminescence spectrum of n-type GaAs:Cr consists of two bands at 0.84 eV (energy position of the O-phonon line) and 0.56 eV when measured at 4.2 K [1]. It has been established that both bands are, in some way, due to Cr centers. Several different models have been reported in the literature [1-4]. Our measurements on Al_xGa_{1-x}As:Cr:Sn crystals favor the Koschel *et al.* [1] and Lin-Chung [3] models describing the 0.84 eV photoluminescence band.

We observed a strong photoluminescence band centered at 0.78 eV in n-type GaAs:Cr:Sn crystals when measured at 77 K. Similar semi-insulating LPE GaAs:Cr crystals, not intentionally doped with shallow donors, gave no detectable peak in this energy range. The carrier concentration in the n-type crystals was $\approx 10^{16} \text{ cm}^{-3}$ and $< 10^{11} \text{ cm}^{-3}$ in the semi-insulating crystals. The melts from which both types of crystals were grown contained 0.5 at.% Cr.

N-type LPE Al_xGa_{1-x}As:Cr:Sn single crystals were grown from melts containing 0.5 at.% of both Cr and Sn. The carrier concentration in these crystals was 10^{16} to 10^{17} cm^{-3} . The energy position of the band-to-band photoluminescence peak was used to establish the Al composition through the relation $E_F = 1.491 + 1.042x + 0.468x^2$. The photoluminescence band due to Cr²⁺ was also observed. This, to our knowledge, is the first observation of the Cr²⁺ photoluminescence peak in Al_xGa_{1-x}As:Cr crystals for x > 0. Figure 1 shows,

as an example, the photoluminescence peak observed for x = 0.42. Peaks for other Al compositions are similar to the one shown here. The energy position of the peak centered at 0.78 eV does not depend on the value of x and is located at the same energy as observed in GaAs:Cr:Sn crystals. The position of this band as a function of x is shown in Fig. 2.

Preliminary results have also been obtained at liquid He temperature from an Al_xGa_{1-x}As:Cr:Sn single crystal with x = 0.23. The photoluminescence spectrum taken at 4.2 K is shown in Fig. 3. A characteristic sharp zero phonon line is observed at 0.825 eV. The corresponding spectrum taken at 77 K is shown for comparison. These data provide experimental evidence that the observed photoluminescence peaks are due to Cr. Systematic photoluminescence measurements at 4.2 K are now under way.

The crystal field splitting of the Cr²⁺ levels is mainly caused by the electrostatic field of nearest neighbor As⁻ ions. It thus follows that the crystal field splitting is almost independent of composition x. Therefore the separation of the ⁵T₂ and the ⁵E levels is approximately the same for all compositions even though the energy gap of the crystal varies with composition. The influence of next nearest neighbors on the crystal field splitting of the Cr²⁺ levels should be evident from our photoluminescence measurements at 4.2 K on Al_xGa_{1-x}As:Cr:Sn crystals with different values of x.

It is tentatively assumed that the energy difference between the Cr²⁺ (⁵T₂) ground level and the bottom of the conduction band increases in proportion to the energy gap of the crystal. This assumption is very well fulfilled by several other deep impurities in Al_xGa_{1-x}As crystals. According to Lang [5, 6], all levels in Al_xGa_{1-x}As except vacancy levels have the same relative shift, E(x)/E(0), with x as the band gap. Using this rule, we conclude in our case that the separation of the Cr²⁺ ground level and the bottom of the conduction band

* Permanent address: Institute of Experimental Physics, Warsaw University, Warsaw, Poland.

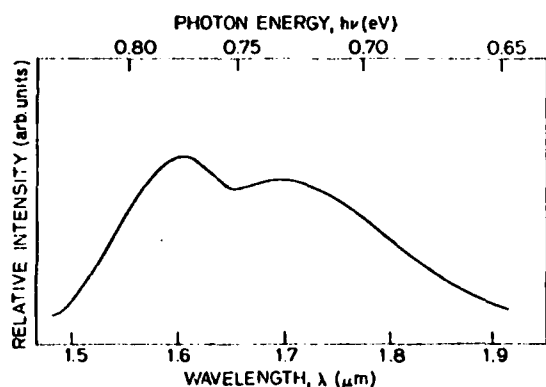


Fig. 1. Photoluminescence peak due to Cr²⁺ in $\text{Al}_x\text{Ga}_{1-x}\text{As}:\text{Cr}:\text{Sn}$ for $x = 0.42$ when measured at 77 K.

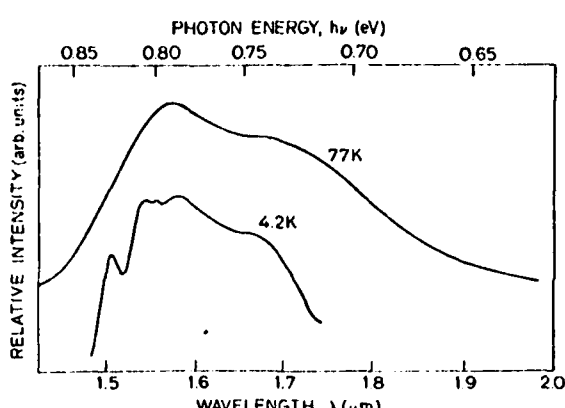


Fig. 3. Photoluminescence peaks due to Cr²⁺ in $\text{Al}_x\text{Ga}_{1-x}\text{As}:\text{Cr}:\text{Sn}$ for $x = 0.23$ when measured at 77 and 4.2 K. The characteristic zero phonon line is at 0.825 eV in the 4.2 K spectrum.

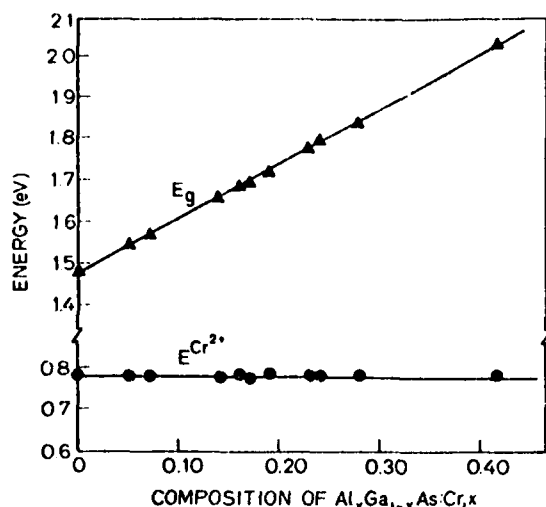


Fig. 2. Dependence of the position of the Cr²⁺ photoluminescence peak and of the energy gap on Al composition x in $\text{Al}_x\text{Ga}_{1-x}\text{As}:\text{Cr}:\text{Sn}$ crystals when measured at 77 K.

should change about 0.3 eV in $\text{Al}_x\text{Ga}_{1-x}\text{As}$ when x changes from 0 to 0.42. Therefore it follows that, if the 0.84 eV photoluminescence band were due to transitions between the bottom of the conduction band and the ground level of Cr²⁺ (Stocker *et al.* model), the energy location of this band would change with x and for $x = 0.42$ the band would be centered at about 1.1 eV. Based on our experimental results and the considerations described above we conclude that the Cr²⁺ photoluminescence peak is due to intraimpurity transitions between the ⁵E and ⁵T₂ crystal field states of Cr²⁺. Precise measurements (transient capacitance and photo-capacitance) of the ionization energy of Cr²⁺ as a function of x are now under way.

Acknowledgements -- We wish to thank B.L. Mattes of the Center for Materials Research at Stanford and our associates at Stanford Electronics Laboratories for many helpful discussions.

REFERENCES

1. KOSCHEL W.H., BISHOP S.G. & McCOMBE B.D., *Solid State Commun.* **19**, 521 (1976).
2. STOCKER H.J. & SCHMIDT M., *Proc. 13th Int. Conf. on the Physics of Semiconductors*, p. 611. Tipografia Marves, Rome (1976).
3. LIN-CHUNG P.J., *Bull. Am. Phys. Soc.* **22**, 599 (1976).
4. OMEL'YANOVSKII E.M., PANTYUKHOV A.N., PERVOVA L.Ya., FISTEL' V.I. & VASIL'EV Yu.A., *Sov. Phys. Semicond.* **9**, 1267 (1976).
5. LANG D.V., LOGAN R.A. & KIMERLING L.C., *Proc. 13th Int. Conf. on the Physics of Semiconductors*, p. 615. Tipografia Marves, Rome (1976).
6. LANG D.V., *Proc. Int. Conf. on Radiation Effects in Semiconductors*, Dubrovnik, Yugoslavia (1976) in press.

APPENDIX C

Properties of Cr deep levels in $\text{Al}_x\text{Ga}_{1-x}\text{As:Cr}$

K. Kocot,* R. A. Rao,[†] and G. L. Pearson

Stanford Electronics Laboratories, Stanford University, Stanford, California 94305

(Received 6 September 1978; revised manuscript received 30 January 1979)

Studies have been conducted which clarify the mechanism producing the 0.8-eV photoluminescent band in $\text{Al}_x\text{Ga}_{1-x}\text{As:Cr}$. Photocapacitance was employed to measure the optical ionization energies of Cr^{2+} with respect to the conduction and valence bands as a function of composition x . It was shown that the sum of the optical ionization energies of Cr^{2+} exceeds the direct energy gap by an amount ΔE , the magnitude of which decreases with increase in x . An explanation of this result is given in terms of the conduction-band structure and Stokes' shift. Photoconductivity measurements were carried out which establish the degeneracy range of the $\text{Cr}^{2+}(E)$ excited level with respect to the conduction band as x is varied from 0 to 0.6. Alternate models of photoluminescent intrimpurity transitions from Cr levels in *n*- and *p*-type crystals are analyzed.

I. INTRODUCTION

Gallium arsenide doped with Cr has been the subject of numerous investigations¹⁻⁵ because of its great technological importance. However, the physical nature of the Cr centers has not been firmly established. The AlGaAs:Cr system may have even greater technical importance [e.g., as the semi-insulating material in metal insulator semiconductor (MIS) field-effect transistor devices].

Photoluminescent studies on $\text{Al}_x\text{Ga}_{1-x}\text{As:Cr}$ single crystals at 77 K have shown^{6,7} that the Cr^{2+} band located at 0.8 eV is independent of Al composition x . This result led us to conclude that this band arises from internal transitions between the 3E excited state and the $^3T_2(\text{Cr}^{2+})$ ground level. The present study was undertaken in order to determine the energy level diagram of the $\text{Al}_x\text{Ga}_{1-x}\text{As:Cr}$ system and to obtain further experimental evidence concerning the nature of the photoluminescent transitions which produce the 0.8-eV band.

II. CRYSTAL GROWTH

The $\text{Al}_x\text{Ga}_{1-x}\text{As:Cr}$ single crystal layers were grown on (100) GaAs substrates using liquid-phase epitaxial (LPE) techniques. High quality crystals of the desired composition ($0 < x < 0.6$) were prepared by adding the required amount of Al to As-saturated Ga melts as specified by the phase equilibria data of Panish and Illegems.⁸ Semi-insulating crystals were obtained by adding 0.5 mole % Cr to the melt and *n*- or *p*-type layers were grown by doping with Sn or Ge.

Prior to growth, the melts were baked out for 50 h at 800 °C in flowing H_2 to remove residual impurities. The melt was then placed on the substrate and an LPE layer, $\approx 5\text{-}\mu\text{m}$ thickness, was grown as the system cooled from 800 to 785 °C. Terminating the growth cycle at 798 °C, provided

$\approx 0.5\text{-}\mu\text{m}$ layers. The semi-insulating layers had differential resistivities in the $10^{10} \Omega \text{ cm}$ range at 1 V, and the carrier concentration in the Sn or Ge doped layers was adjusted to $1-5 \times 10^{16} \text{ cm}^{-3}$.

III. PHOTOCAPACITANCE MEASUREMENTS

Electron-spin resonance studies⁹⁻¹¹ have shown that Cr can be present in three different charge states in GaAs. These include Cr^{3+} , Cr^{2+} , and Cr^+ ions which are in order (i) neutral, (ii) single negatively and (iii) double negatively charged with respect to the lattice.

Photocapacitance measurements were carried out in order to determine the location of the Cr^{2+} ground level within the energy gap of $\text{Al}_x\text{Ga}_{1-x}\text{As:Cr}$ and its dependence on composition x . A double source photocapacitance technique, as described by White *et al.*,¹² was used for this purpose. Schottky barrier diodes were prepared by evaporating small Au dots on (*n*) $\text{Al}_x\text{Ga}_{1-x}\text{As:Cr}$ single-crystal layers and breaking down one of the dots to form an ohmic contact.

The sample was irradiated simultaneously with light at both the prime and probe energies. The prime energy was fixed slightly below the band gap while the probe energy was varied to excite the various levels under investigation (0.7 to 2.2 eV in our studies). The prime light creates a fixed population of holes on the Cr^{2+} levels which, in accordance with the transition probabilities and relevant rate equations, produces a steady state capacitance. This capacitance is altered as the second light source (probe radiation) is swept from low to high energies. Above the ionization energy of Cr^{2+} or Cr^+ the probe light upsets the steady state populations by transfer of carriers to the conduction or valence band, respectively. These carriers are swept away by the electric field at the depletion region, thus altering the space charge distribution so that the capacitance changes to a

new value, greater or smaller according to whether the transitions are to the conduction or valence band.

A typical photocapacitance spectrum of an *n*-type $\text{Al}_x\text{Ga}_{1-x}\text{As:Cr}$ crystal is shown in Fig. 1 as measured at 85 K. Two thresholds are observed which we assign to Cr levels. This assignment is based on the fact that the thresholds appear only in Cr doped samples, and that they are located in the expected energy range. The negative change of capacitance corresponds to transition of holes from the Cr^{3+} level to the valence band, and its threshold gives the position of the Cr^{3+} level with respect to the top of the valence band. The positive change of capacitance corresponds to the transfer of electrons from the Cr^{3+} level to the conduction band and its threshold gives the location of the Cr^{2+} level with respect to the conduction band. The measured value is dependent on the relative positions of the Γ and L minima as will be discussed in Sec. V.

The thresholds of electronic transitions from the Cr^{3+} ground level to the conduction band are shown in Fig. 2(a) for crystals having different values of x . It is seen that the optical ionization energies vary from 0.80 to 1.00 eV when x varies from 0 to 0.42. Figure 2(b) shows the thresholds of hole transitions from the Cr^{3+} ground level to the top of the valence band as obtained from the same set of crystals. In this case the optical ionization energies vary from 0.90 to 1.20 eV. A summary of the data together with the Γ and L band gap energies are given in Table I.

It is to be noted that the sum of the ionization energies at each value of x exceeds the direct bandgap E_x^Γ by an amount ΔE . This excess, as plotted versus crystal composition in Fig. 3, decreases with x but levels off around 0.3. This behavior will be discussed in Sec. V.

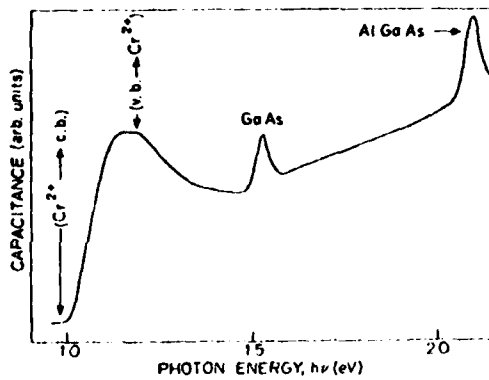


FIG. 1. Photocapacitance spectrum of *n*-type $\text{Al}_{0.42}\text{Ga}_{0.58}\text{As:Cr}$ at 85 K. The structure between 1.0 and 1.3 eV arises from the Cr^{3+} level.

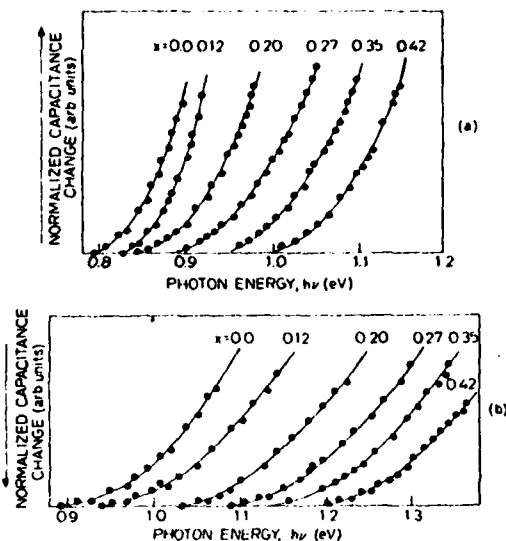


FIG. 2. Photoionization thresholds of the Cr^{2+} level in (*n*) $\text{Al}_x\text{Ga}_{1-x}\text{As:Cr}$. (a) Conduction band and (b) valence band. Note that the ordinate scale is reversed in (b).

Similar photocapacitance measurements were carried out on *p*-type crystals. Since it was impossible to make satisfactory Schottky barriers on this material, the measurements were made on grown (*p*) $\text{Al}_x\text{Ga}_{1-x}\text{As:Cr}$ - (*n*) GaAs heterojunctions. Thresholds were observed at the same energies as

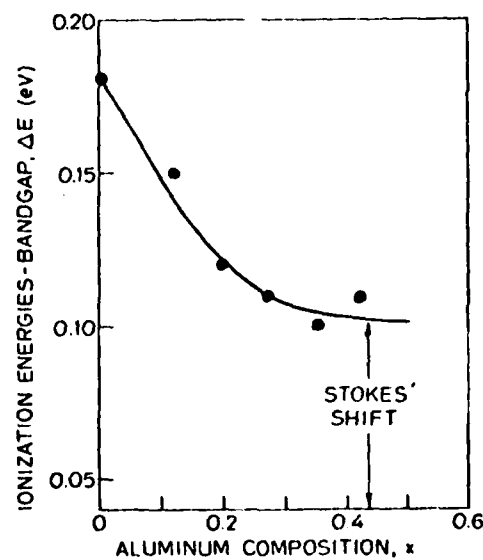


FIG. 3. Sum of the optical ionization energies of Cr^{2+} minus the band gap energy vs x .

TABLE I. Optical ionization energies of Cr with respect to the valence and conduction bands at 85 K. (All energies are given in electron volts.)

x^a	Cr ²⁺ – valence band ^b	conduction band – Cr ²⁺ ^c	ΣE_I^d	E_I^{Γ} ^e	E_I^L ^f	ΔE^g
0	0.90	0.80	1.70	1.52	1.71	0.18
0.12	0.99	0.83	1.82	1.67	1.79	0.15
0.20	1.04	0.85	1.89	1.77	1.84	0.12
0.27	1.09	0.89	1.98	1.87	1.89	0.11
0.35	1.14	0.94	2.08	1.98	1.93	0.10
0.42	1.20	1.00	2.20	2.09	1.98	0.11

^a Al composition of $\text{Al}_x\text{Ga}_{1-x}\text{As:Cr}$ crystal.

^b Ionization energy of Cr²⁺ with respect to the valence band.

^c Ionization energy of Cr²⁺ with respect to the conduction band.

^d Sum of the ionization energies.

^e Band gap at the Γ point.

^f Band gap at the L point (295 K).

^g $\Sigma E_I - E_I^{\Gamma}$.

in *n*-type $\text{Al}_x\text{Ga}_{1-x}\text{As:Cr}$, but the direction of capacitance change was reversed. Increase of capacitance in *p*-type crystals is caused by hole emission from the Cr²⁺ center, while transitions from the Cr²⁺ level to the conduction band (electron emission) are observed as a decrease in capacitance.

IV. PHOTOCONDUCTIVITY MEASUREMENTS

Photoconductivity measurements were carried out in order to determine the composition range in which the Cr²⁺(⁵E) excited level is degenerate with the conduction band and also to verify the optical ionization energies obtained from our photocapacitance measurements.

N-type $\text{Al}_x\text{Ga}_{1-x}\text{As:Cr}$ LPE layers with selected Al compositions were grown on high resistivity undoped GaAs substrates. Ohmic contacts were applied to the conduction layer by alloying In pellets.

The photoconductivity spectra shown in Fig. 4 were recorded from crystals having compositions $0.0 \leq x \leq 0.6$. The peaks centered around 0.95 eV are due to ³T₂(Cr²⁺) → ⁵E transitions; those at 1.5 eV are from band-to-band transitions in the GaAs substrate and those at higher energies from band-to-band transitions in the AlGaAs layer. Note that the Cr peaks are present in crystals with $x = 0$, 0.12, and 0.23 but are absent when $x = 0.38$ and 0.60. The ⁵E excited level must therefore be within the conduction band when $x \leq 0.23$ and within the band gap when $x \geq 0.38$.

V. DISCUSSION

This section will discuss the dependence of the ionization energies of Cr²⁺ on Al composition, the degeneracy of the ⁵E(Cr²⁺) excited level, and alternate models for describing photoluminescent

intrairmpurity transitions in AlGaAs:Cr.

It was mentioned in Sec. III that the sum of the optical ionization energies with respect to the valence and conduction bands exceeds the direct energy gap by an amount ΔE . The relationship be-

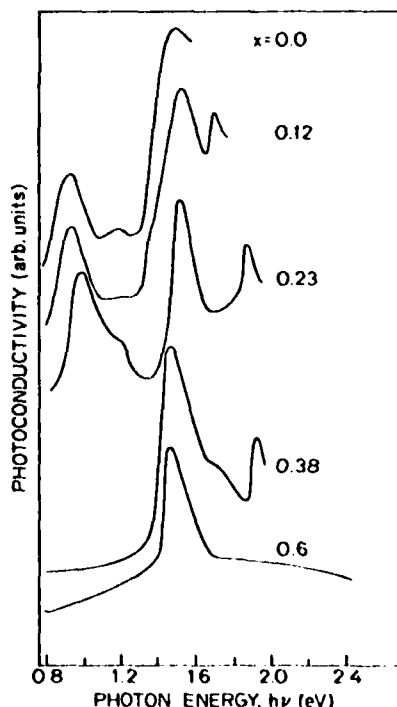


FIG. 4. Photoconductivity spectra of (n) $\text{Al}_x\text{Ga}_{1-x}\text{As:Cr}$ at 85 K. The peaks located near 0.95 eV are due to Cr²⁺ internal transitions.

tween ΔE and Al compositions x , as shown in Fig. 3, can be explained by the conduction band structure of $\text{Al}_x\text{Ga}_{1-x}\text{As}:\text{Cr}$ after taking the Stokes shift into account. The L minimum is 0.19 eV above the Γ minimum in GaAs. The Cr level is highly localized in real space and hence is delocalized (spread out) in k space so that optical transitions are possible to the L minimum. Since the density of states in the Γ minimum is much smaller than in the L minimum, only the higher-energy regions of the valley contribute to the photocapacitance change. Even at $x=0$ the change of capacitance as a result of transitions to the L minimum is larger than that due to transitions to the Γ minimum. As x increases, the Γ minimum moves up in energy faster with respect to the valence band than the L minimum and both have approximately the same value at $x=0.4$. Beyond this point $\text{Al}_x\text{Ga}_{1-x}\text{As}:\text{Cr}$ becomes an indirect gap material. It thus follows that the energy involved in optical transitions from the Cr^{2+} ground level to the conduction band should increase rapidly at first as x increases from zero but approach a constant value as we approach and pass $x=0.4$.

The DLTS measurements of Lang and Logan on $\text{GaAs}:\text{Cr}$ ¹³ have shown that the thermal ionization energy of transitions from Cr^{2+} to the bottom of the conduction band is 0.61 eV. Hence, at $x=0$, the energy involved in optical transitions into the conduction band should have an intermediate value between 0.61 eV (Γ valley) and 0.80 eV (L valley) which is consistent with the value of 0.80 eV ($\Delta E = 0.18$ eV) given in Table I. Based on these considerations, ΔE is expected to approach 0 as x approaches 0.4. However, a contribution from the Stokes shift causes ΔE to level off at 0.1 eV as indicated in Fig. 3. It should be noted that the thermal excitation energy of $\text{GaAs}:\text{Cr}$ plus its optical ionization energy to the top of the valence band is equal, as expected, to the direct bandgap energy ($E_g^r = 1.52$ eV at 85 K).

From the above analysis and the experimental results presented in this paper, we have drawn the energy level diagram shown in Fig. 5. The solid data points give the position of the ${}^3T_2(\text{Cr}^{2+})$ ground level with respect to the conduction band as obtained from photocapacitance thresholds, and the open circles indicate the energy position of the 3E excited level as obtained from photoconductivity peaks. The dashed portion of the curve has been extrapolated beyond the region where measurements were possible. It can be seen that the $\text{Cr}^{2+}({}^3E)$ excited level is a resonant state (degenerate) in $\text{Al}_x\text{Ga}_{1-x}\text{As}:\text{Cr}$ crystals when x is less than ≈ 0.35 but is a discrete state (a state lying within the band gap) when x is greater than this value.

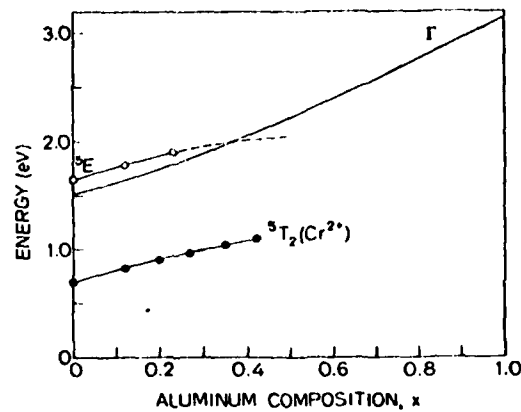


FIG. 5. Energy level diagram of $\text{Al}_x\text{Ga}_{1-x}\text{As}:\text{Cr}$. ● from photocapacitance data, ○ from photoconductance data—extrapolation.

The results presented in Ref. 6 together with the photocapacitance and photoconductivity data given above prove that the 0.8-eV photoluminescent peak in $\text{Al}_x\text{Ga}_{1-x}\text{As}:\text{Cr}$ is due to intrairimpurity transitions.

The models shown in Fig. 6 are proposed to explain internal field transition in both n - and p -type $\text{AlGaAs}:\text{Cr}$ crystals. The Cr atoms occupy Ga or Al sites and therefore appear in the 3^+ charge state in high purity crystals. However, compensation exists in n -type material containing shallow donors which converts Cr to the 2^+ charge state. Electrons are excited from the $\text{Cr}^{2+}({}^3T_2)$ ground level to the conduction band by laser light to produce Cr in the 3^+ charge state and an electron in the conduction band. The Cr^{3+} center then captures

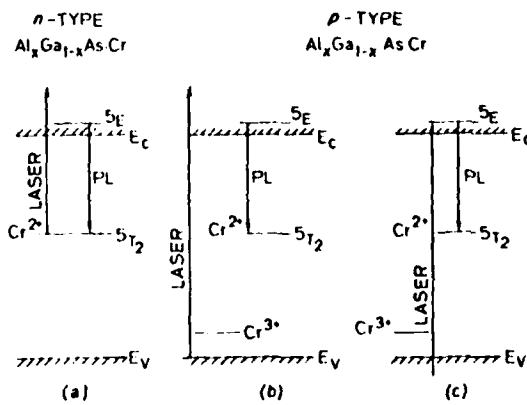


FIG. 6. Possible excitation mechanisms of photoluminescence in n - and p -type $\text{Al}_x\text{Ga}_{1-x}\text{As}:\text{Cr}$ crystals based on crystal-field theory.

an electron to produce a Cr^{2+} center in the 3E excited state which decays radiatively to emit the photoluminescent signal as shown in Fig. 6(a).

In *p*-type AlGaAs:Cr , electrons are excited from the valence to the conduction band and then captured by the Cr^{4+} centers to produce a Cr^{2+} center in the 3E excited state which, as in *n*-type crystals, decays radiatively to give the 0.8-eV photoluminescent peak [Fig. 6(b)]. A second mechanism is also possible in *p*-type crystals. Electrons are excited by the laser light from within the valence

band to the 3E excited state of Cr^{2+} and then decay radiatively to the 3T_2 ground level to produce the photoluminescent peak as shown in Fig. 6(c).

Probably each of the described mechanisms contributes to the 0.8-eV photoluminescent band in *p*-type AlGaAs:Cr .

ACKNOWLEDGMENT

This work was supported by the Office of Naval Research, Contract N00014-78-C-0297.

*Present address: Institute of Experimental Physics, Warsaw Univ., Hoza 69, Warsaw, Poland.

†Present address: Dept. of Electrical Engineering, San Jose State Univ., San Jose, Calif. 95192.

¹W. H. Koschel, S. G. Bishop, and B. D. McCombe, Solid State Commun. **19**, 521 (1976).

²A. L. Lin and R. M. Bube, J. Appl. Phys. **47**, 1959 (1976).

³H. J. Stocker and M. Schmidt, *Proceedings of the Thirteenth International Conference on the Physics of Semiconductors* (Tipografia Marves, Rome, 1976), p. 611.

⁴E. C. Lightowers and C. M. Penchina, J. Phys. C **11**, L405 (1978).

⁵L. Instone and L. Eaves, J. Phys. C **11**, L771 (1978).

⁶K. Kocot and G. I. Pearson, Solid State Commun. **25**, 113 (1978).

⁷V. F. Kovalenko, F. P. Kesamanly, J. E. Maronchuk,

B. P. Masenko, G. P. Peka, and L. G. Shepel, Sov. Phys. Semicond. **11**, 1303 (1977).

⁸M. B. Panish and M. Hegemus, in *Progress in Solid-State Chemistry*, edited by H. Reiss and J. O. McClain (Pergamon, Oxford, England, 1972), p. 39.

⁹V. Kaufmann and J. Schneider, Solid State Commun. **20**, 143 (1976).

¹⁰G. H. Strauss and J. J. Krebs, in *Gallium Arsenide and Related Compounds (Edinburgh)*, 1976 (Institute of Physics Conference Series No. 33a, Bristol and London, 1977), p. 84.

¹¹J. J. Krebs and G. H. Strauss, Phys. Rev. B **15**, 17 (1977).

¹²A. M. White, P. J. Dean, and P. Porteous, J. Appl. Phys. **47**, 3230 (1976).

¹³D. V. Lang and R. A. Logan, J. Electron. Mater. **4**, 1053 (1975).

APPENDIX D

PREPARATION AND PROPERTIES OF $\text{Al}_x\text{Ga}_{1-x}\text{As}:\text{Cr}$
SINGLE CRYSTALS

July 1979

Quarterly Report
Covering the Period 1 April 1979
through 30 June 1979

Prepared under
Office of Naval Research
Contract Number N00014-78-C-0297

Solid-State Electronics Laboratory
Stanford Electronics Laboratory
Stanford University Stanford, California

FOREWARD

This is the sixth quarterly report on Stanford Project 5128,
"Preparation and Properties of $\text{Al}_x\text{Ga}_{1-x}\text{As:Cr}$ Single Crystals". The
research was conducted at the Solid-State Electronics Laboratories
by the following personnel:

Professor Gerald L. Pearson: Principal Investigator

Maurice Landstrass: Staff

I. Objective

The objective of this research program is to prepare semi-insulating $\text{Al}_x\text{Ga}_{1-x}\text{As}:\text{Cr}$ epilayers for use in studying the interface properties of $\text{Al}_x\text{Ga}_{1-x}\text{As}:\text{Cr}/\text{GaAs}$ heterojunctions and to determine the utility of this system for MISFET applications.

II. Materials and Device Preparation

A total of 12 device structures were prepared during the past quarter. All epitaxial layer structures were grown by LPE techniques. The emphasis in this phase of the program was to define the growth procedures required for reproducible growth of highly compensated $\text{Al}_{0.5}\text{Ga}_{0.5}\text{As}:\text{Cr}$ epilayers. The independent parameters investigated were the time and temperature of the melt bakeout preceding crystal growth.

A growth run consisted of first loading two Ga melts into the growth system, one melt was undoped and the other contained nominally 0.47 at % Cr. These melts were then baked in flowing H_2 for a prescribed time and temperature. The furnace was then cooled and Al metal, undoped polycrystalline GaAs, and an (n^+)GaAs:Te substrate were loaded into the system. The furnace was then heated to 800°C for two hours before starting growth. Each grown device consisted of a 4 micron thick layer of GaAs(n -type $n \approx 10^{15} - 10^{16} \text{ cm}^{-3}$) and a 0.8 micron layer of $\text{Al}_{0.5}\text{Ga}_{0.5}\text{As}:\text{Cr}$. Our study of the melt bakeout conditions defined the compensated growth regime as the temperature interval between 486 and 500°C. Regardless of bakeout time, melts baked out at temperatures below this interval always produced n-type

$\text{Al}_{0.5}\text{Ga}_{0.5}\text{As:Cr}$ layers and melts baked above this interval always produced p-type $\text{Al}_{0.5}\text{Ga}_{0.5}\text{As:Cr}$ layers. The effect of bakeout time within the compensated interval was observed to affect the electrical uniformity of the layers. The best results to date have come from melts baked out in the interval between 488 and 490°C.

The layers were characterized by optical and scanning electron microscopy. Figure 1 shows SEM photomicrographs of sample 917 at two different magnifications. As can be seen from Fig. 1b, the metallurgical $\text{Al}_{0.5}\text{Ga}_{0.5}\text{As:Cr}/\text{GaAs}$ interface is abrupt and no precipitates are observable in the $\text{Al}_{0.5}\text{Ga}_{0.5}\text{As:Cr}$ layer. As determined from Fig. 1a, the thickness of the GaAs layer is 4.65 microns and that of the $\text{Al}_{0.5}\text{Ga}_{0.5}\text{As:Cr}$ layer is 0.79 microns.

III. Electrical Measurements

I-V measurements were performed using a Keithly 610 electrometer in the feedback mode. Fig. 2 is a plot of the I-V characteristics of an MIS diode made from wafer No. 917. Assuming that the current is dominated by the resistance of the $\text{Al}_{0.5}\text{Ga}_{0.5}\text{As:Cr}$ layer, the data from the ohmic range of the characteristic yield a bulk resistivity of 1.4×10^{11} ohm-cm.

Capacitance and conductance versus voltage measurements were made at 1 kHz, 10 kHz and 1 MHz (point by point) using an H-P 4270 Automatic Capacitance Bridge. Capacitance versus voltage characteristics were also measured at 1 MHz with a Boonton 72B capacitance meter while the gate voltage was swept at 0.2 V/sec. Fig. 3 exhibits point by point plots of the C-V characteristics of a diode from

wafer No. 917 taken at 1 kHz, 10 kHz and 1 MHz. Figure 4 is a plot of the 1 MHz characteristic (measured on the Boonton meter) measured on the same device 2 days prior to the measurements of Figs. 2 and 3.

As can be seen by comparison of Figs. 3 and 4, the device characteristics at 1 MHz have altered significantly. The major difference is that Fig. 4 exhibits a flat characteristic at large negative biases whereas Fig. 3 shows non-equilibrium MIS behavior.

It was also observed that the device current at all voltages increased with time. This is consistent with the change observed in the C-V characteristic. Etching and annealing experiments of the degraded devices were not successful in restoring the characteristics.

IV. Conclusions

Work to date has focussed on the development of procedures for the growth of semi-insulating $\text{Al}_{0.5}\text{Ga}_{0.5}\text{As:Cr}$ layers. Layers having resistivities of 1.4×10^{11} ohm-cm have been grown by this technique. Electrical measurements on devices prepared from these crystals indicate that the insulating properties of such layers are sufficient for MIS behavior to be observed.

Work during the next quarter is planned to produce a continuous supply of high resistance layers. These will be used in detailed electrical studies of the interface. These programs will proceed in parallel with refinements of the growth procedures that include the effect of bakeout time.

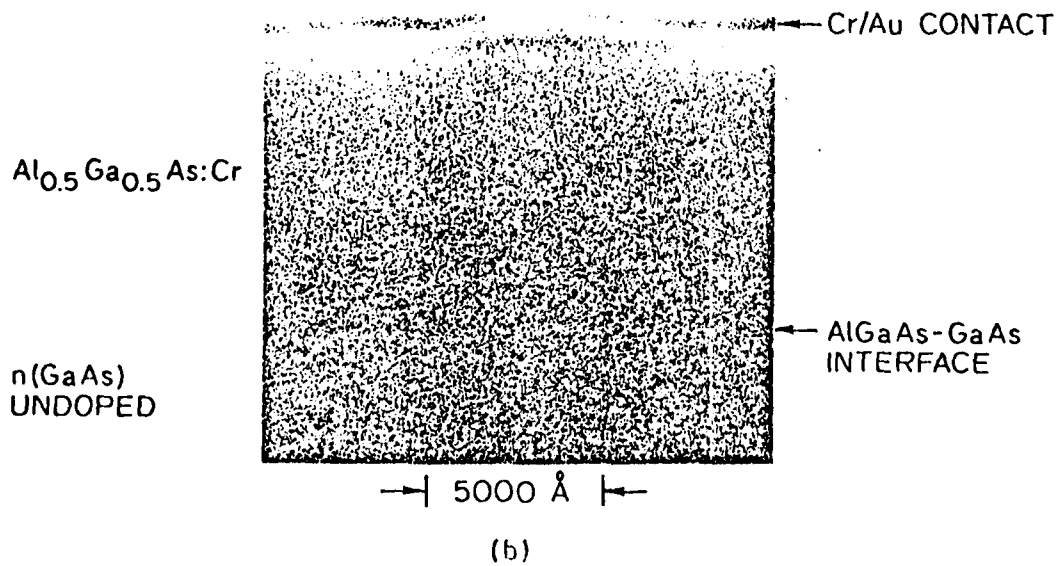
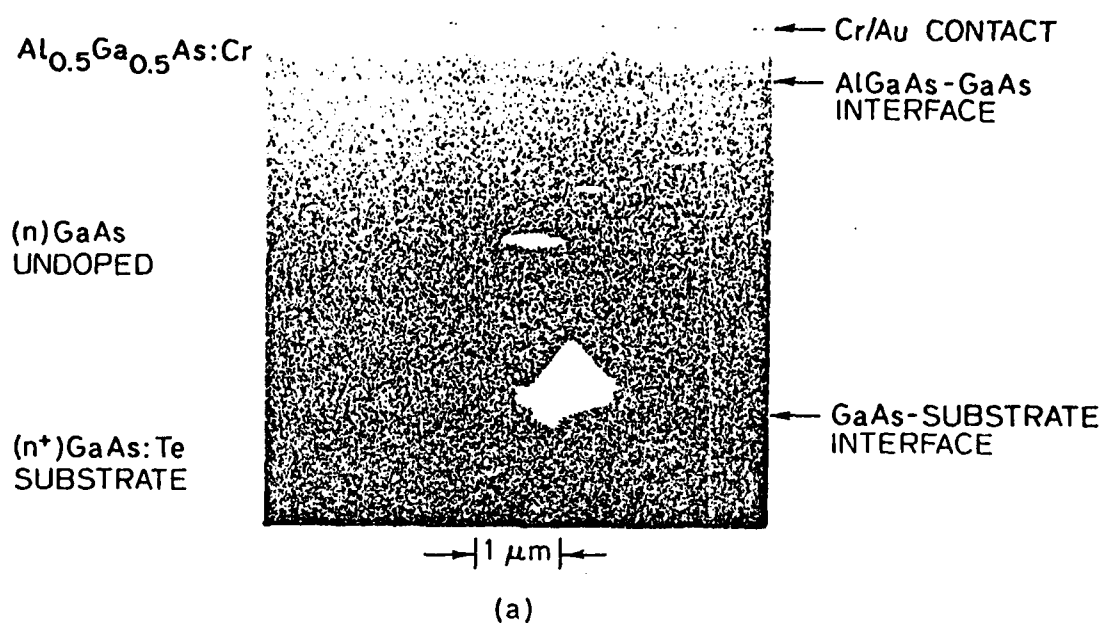


Fig. 1 SEM Photomicrographs of a Cleaved Au/Cr-Al_{0.5}Ga_{0.5}As:Cr-(n)GaAs Diode

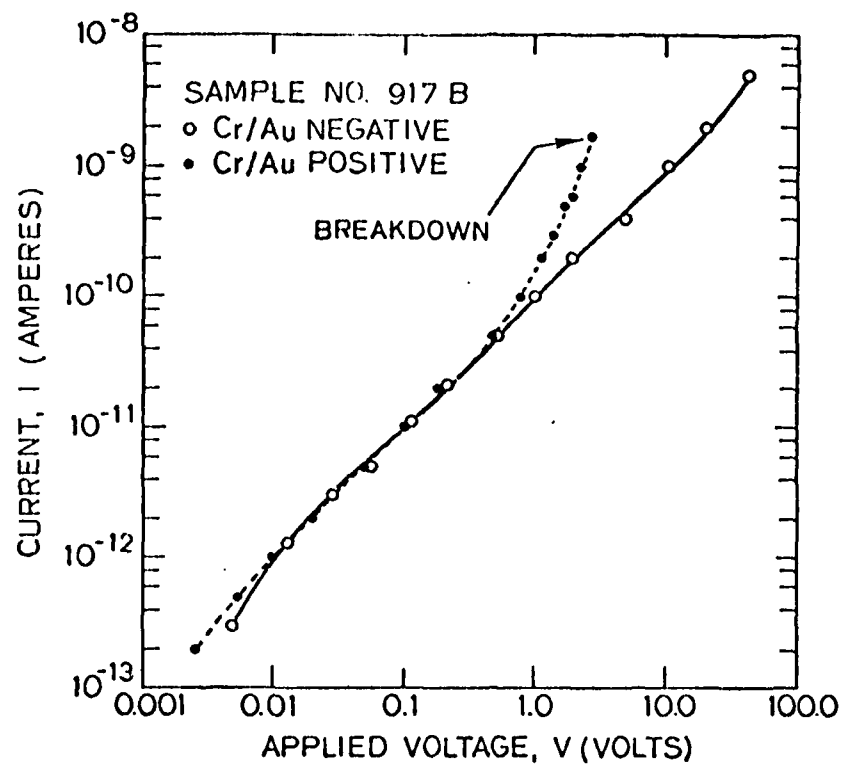


Fig. 2. I-V Characteristics of $\text{Au/Cr-Al}_{0.5}\text{Ga}_{0.5}\text{As:Cr-(n)GaAs}$ Diode. Area = 1.13 cm^{-2} and AlGaAs Layer Thickness = 8000 \AA .

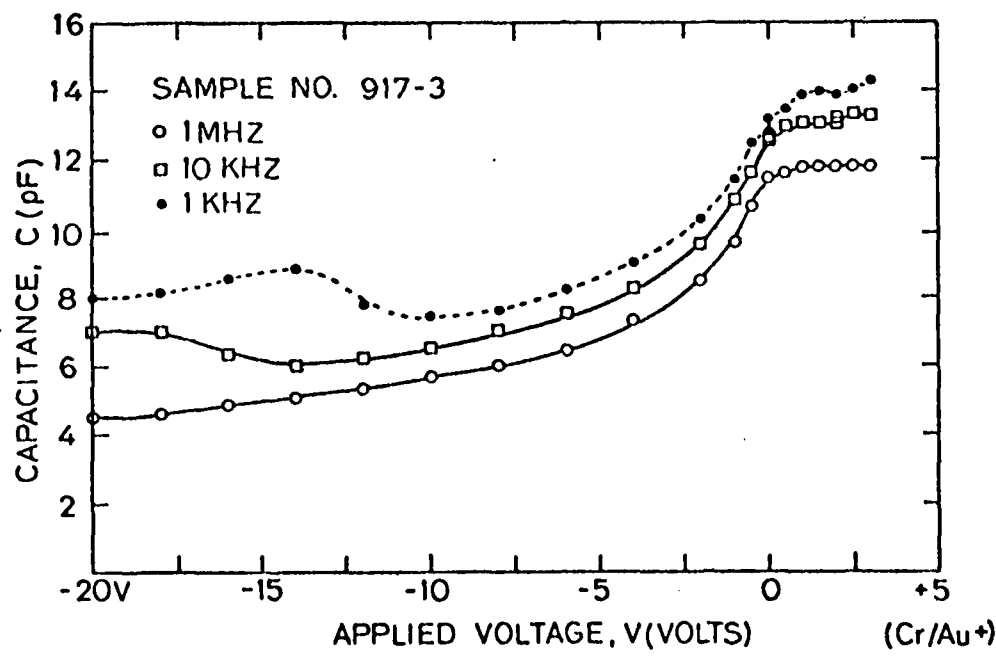


Fig. 3. C-V Characteristics of $\text{Au/Cr-Al}_{0.5}\text{Ga}_{0.5}\text{As:Cr-(n)GaAs}$ Diode. The Independent Variable is Frequency. Area = $1.13 \times 10^{-3} \text{ cm}^2$.

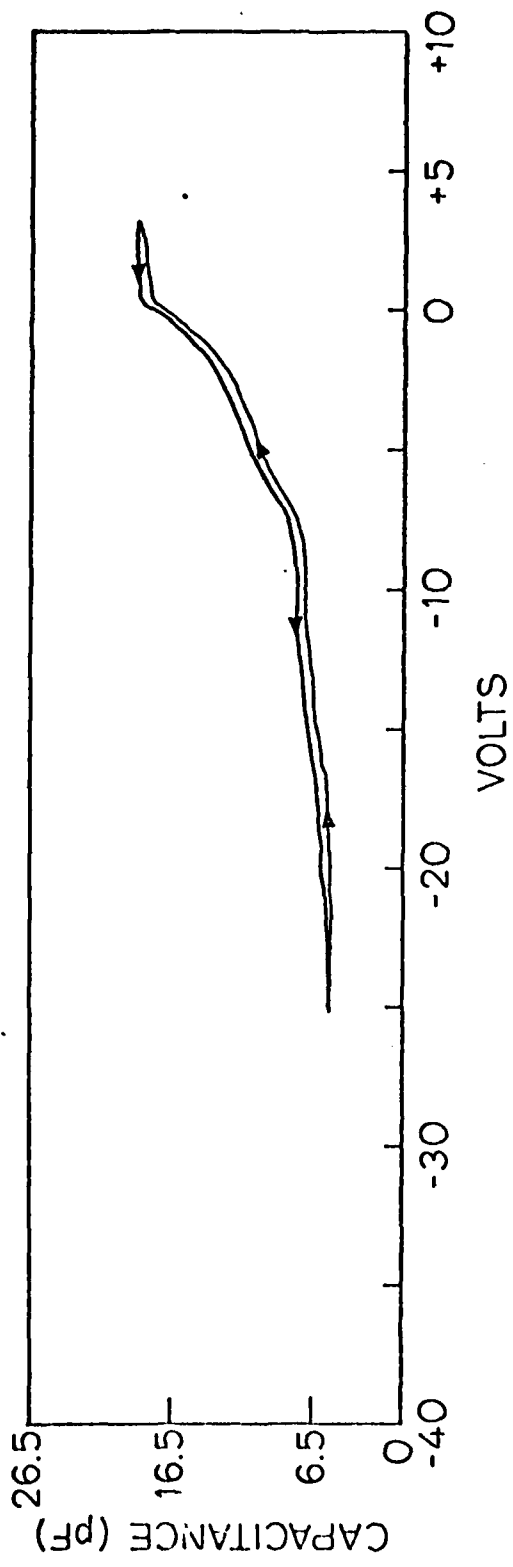


Fig. 4 C-V Characteristic of Diode Used in Fig. 3. The Recorder Tracing Was Made at 1 MHz with a Boonton 72B Capacitance Meter Swept at 0.2 V/sec. This Plot Was Obtained Two Days Prior to That of Fig. 3.

APPENDIX E

PREPARATION AND PROPERTIES OF $\text{Al}_x\text{Ga}_{1-x}\text{As:Cr}$
SINGLE CRYSTALS

October 1979

Quarterly Report
Covering the Period 1 July 1979
through 30 September 1979

Prepared under
Office of Naval Research
Contract Number N00014-78-C-0297

Solid-State Electronics Laboratory
Stanford Electronics Laboratories
Stanford University Stanford, CA 94305

FOREWORD

This is the seventh quarterly report on Stanford Project J-528, "Preparation and Properties of $\text{Al}_x\text{Ga}_{1-x}\text{As:Cr}$ Single Crystals". The research was conducted at the Solid-State Electronics Laboratories by the following personnel:

Professor Gerald L. Pearson: Principal Investigator
Maurice Landstrass: Staff

I. Objective

The objective of this research program is to prepare semi-insulating $\text{Al}_x\text{Ga}_{1-x}\text{As:Cr}$ epi-layers for use in studying the interface properties of $\text{Al}_x\text{Ga}_{1-x}\text{As:Cr-GaAs}$ heterojunctions and to determine the utility of this system for MISFET applications.

II. Materials and Device Preparation

Work in this area was focussed on refinements of the crystal growth procedures with respect to bakeout time of the Ga and Ga:Cr melts. The melt bakeout temperature was varied from 460 to 495°C and the melt bakeout time was varied between 17 and 70 hours.

The overall result from this study was that, as the bakeout time increased from 17 to 70 hours, the nominal temperature of the bakeout necessary for growth of compensated layers decreased from 490 to 478°C. Crystals grown from melts baked out at temperatures above this interval were p-type and below were n-type. This result indicates that the major effect of bakeout time is to reduce the n-type impurity content of the melt by a process which is kinetically limited but not strongly thermally activated. In contrast, the incorporation of p-type impurities is strongly thermally activated.

This last conclusion is supported by multiple growth experiments from the same melt where it was found that successive growth which produced partially compensated n-type crystals during the first run always produced partially compensated p-type crystals even with saturation periods as short as 50 minutes.

III. Electrical Measurements

Electrical studies consisted of capacitance versus voltage measurements at 1 MHz performed as a function of gate voltage sweep rate, temperature, light intensity and spectral content. Capacitance versus voltage measurements were also performed as a function of frequency at room temperature. In addition, I-V measurements taken as a function of temperature, light intensity and spectral content as well as frequency.

The MIS diodes were fabricated from wafers consisting of an 8000 Å thick $\text{Al}_{0.5}\text{Ga}_{0.5}\text{As:Cr}$ layer grown on top of a 4 micron thick GaAs layer having a nominal electron density of $1 \times 10^{16}/\text{cc}$. This heterojunction was grown on top of a 450 micron thick (n^+) GaAs:Te substrate. Diodes were fabricated by evaporating Au-Ge/Ni on the substrate and $1 \times 10^{-3} \text{ cm}^2$ Au/Cr dots on the $\text{Al}_{0.5}\text{Ga}_{0.5}\text{As:Cr}$ layer. The underlying Cr layer was $\approx 300 \text{ \AA}$ and the Au layer was $\approx 2000 \text{ \AA}$.

Figure 1 is a reproduction of a C-V trace obtained at 1 MHz as the gate voltage was swept at .2 V/sec with the sample in the dark at room temperature and in vacuum. The key feature of this characteristic is that the maximum capacitance occurs at negative 0.8 volts. It was found experimentally that samples having maximums in the range from 0.5 to 1.0 volts negative all had similar characteristics. These comprised the group of samples studied in detail during this quarter. An analysis of this characteristic shows that the GaAs layer at the heterojunction interface is slightly accumulated at zero bias and that the $\text{Al}_{0.5}\text{Ga}_{0.5}\text{As:Cr}$ is fully depleted but has a slightly varying capacitance with respect to voltage.

Figures 2 and 3 are log log plots of the I-V characteristics taken at room temperature in vacuum, showing the effect of light on these devices.

The main features of these curves are that (for both polarities) the sharply rising current characteristic saturates at a constant current step. This part of the characteristic has a field emission type I-V characteristic ($I \propto V^2 \exp(-b/V)$), indicating high fields at the heterojunction which causes Fowler-Nordheim type tunneling to be the current controlling mechanism in the device.[1] In this mechanism the current is controlled by the tunneling probability and the thermal generation rate of carriers in the GaAs layer. A constant current step occurs in the characteristic when the device current is limited by the supply of carriers in the GaAs layer. This indicates the onset of nonequilibrium behavior.[2,3] It is found that, in the dark, this constant current step occurs when the Fermi level at the heterojunction interface moves into either the conduction band for positive Au/Cr bias, or into the valence band for negative Au/Cr bias. Figures 2 and 3 show the effect of 8000 Å light on the I-V characteristics. Light of this energy is absorbed only in the GaAs layer. The family of curves in the figures are generated by starting off with the full output of the monochromator and then successively attenuating the output with neutral density filters. Here $I_{\text{max}}/I_{\text{incident}} = 10^{(\text{filter number})}$. The result shows that the current in the step is controlled by the generation rate of carriers in the GaAs layer. In the dark the thermal generation rate is controlling while in the light the optical generation rate is controlling.

In the Cr negative characteristic, the lateral shift in the steeply rising part of the characteristic is caused by the action of light flattening the bands in the GaAs layer. For this MIS diode under maximum illumination the positive and negative characteristics nearly superimpose in the steeply rising current region. For diodes having a flat band voltage

approximately 0.2 volts more positive, the characteristics superimpose in the dark.

The combined results of the I-V and C-V measurements indicate that for devices having nominally the band structure indicated above, it is not possible to increase the field across the Al_{0.5}Ga_{0.5}As:Cr layer past the point where either heavy accumulation or inversion should occur. Non-equilibrium conditions prevail beyond this field. As noted before, this effect is strongly dependent on the point of maximum capacitance and preliminary measurements indicate that the barrier to current flow increases as this point becomes more positive, consistent with the devices reported in the last quarterly report.

The results of I-V measurements with temperature as the independent parameter indicate that, under low bias conditions, the current in these devices is controlled by ohmic conduction in the Al_{0.5}Ga_{0.5}As:Cr layer, yielding a resistivity of ~ 10¹¹ ohm-cm.

The affect of temperature on the 1 MHz C-V characteristics indicates that the variation in capacitance at bias voltages more positive than the point of maximum capacitance is controlled by charging of the Al_{0.5}Ga_{0.5}As:Cr rather than modulation of the depletion region in this layer. This is supported by measurements at 77°K which yield a perfectly flat characteristic in this bias range when the voltage is swept in the positive direction.

The measurements of capacitance versus frequency support the above results in that they indicate nonequilibrium behavior at voltages where either heavy accumulation or inversion should occur. The results to date suggest that, for bias voltages which should modulate the position of the Fermi level within the GaAs bandgap at the interface, equilibrium behavior

is observed. Preliminary analysis of the results indicate strong charging effects in the device that peak when the Fermi level crosses the middle of the GaAs bandgap at the interface. These states begin to respond at 1 kHz, the lowest measurement frequency used to date.

The major conclusion drawn from data taken this quarter is that, with $\text{Al}_{0.5}\text{Ga}_{0.5}\text{As:Cr}$ layers, it is possible to create high electric fields at the GaAs surface. Due to the magnitude of the device currents it was not possible to study accumulation or inversion properties in these samples. Tentative results indicate that useful information regarding the nature of the interface can be obtained from these devices by an equilibrium analysis. Work during the next quarter will focus on the effects of band structure on controlling the current through the device in order to extend the analysis to higher insulator fields.

REFERENCES

1. Z. A. Weinberg, Solid-State Electron. 20, 111 (1977).
2. S. Davidoff, I. Kashat and N. Klein, Appl. Phys. Lett. 34, 782 (1979).
3. P. M. Solomon, Appl. Phys. Lett. 30, 597 (1977).

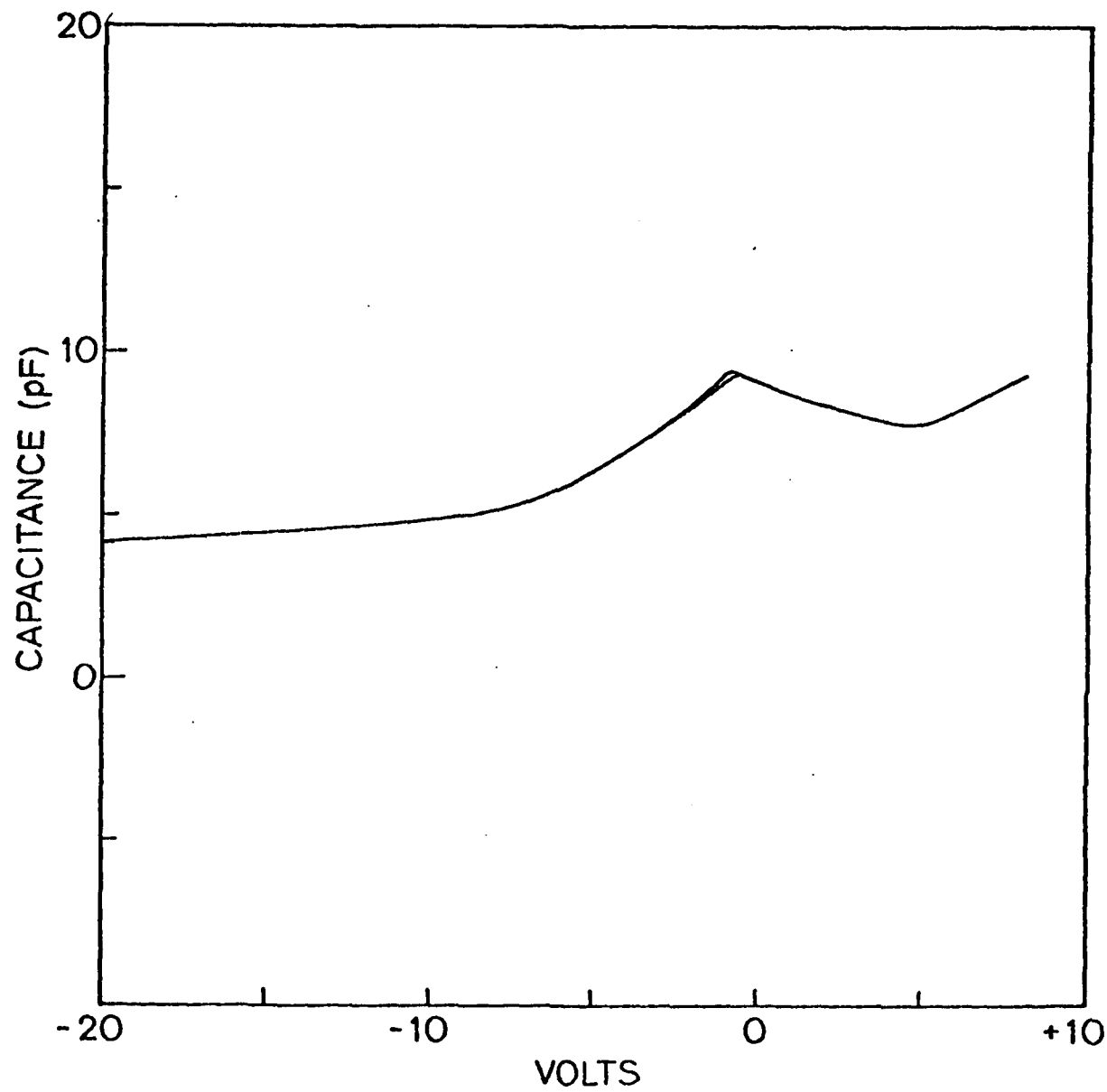


Fig. 1 Capacitance-voltage behavior for a $1 \times 10^{-3} \text{ cm}^2$ area $\text{Au/Cr-Al}_{0.5}\text{Ga}_{0.5}\text{As:Cr-GaAs}$ MIS capacitor. The voltage refers to the polarity of the Au/Cr dot. The measurement was performed at room temperature, in darkness and in vacuum. The bias voltage was swept at 0.2 V/sec.

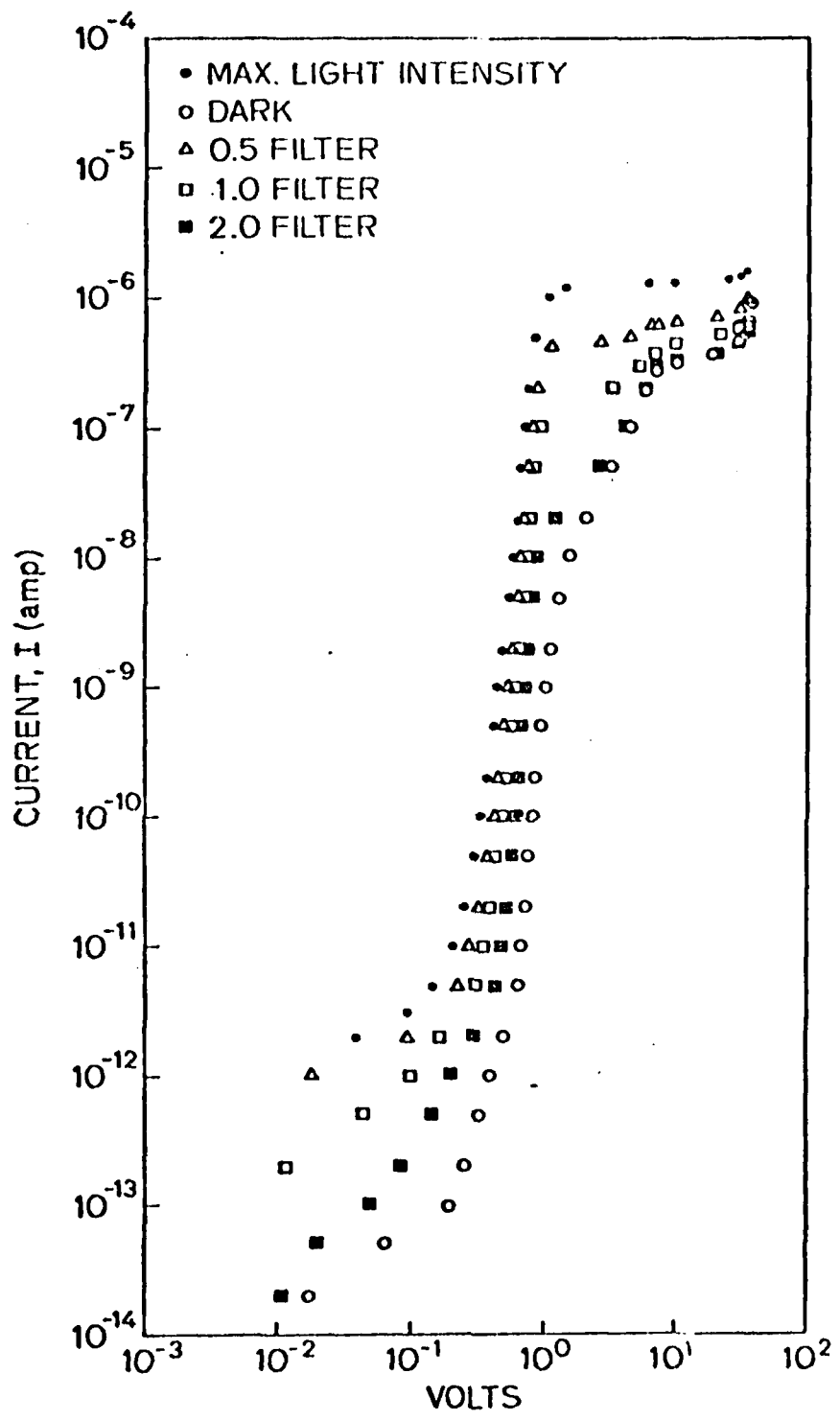


Fig. 2 Current-voltage behavior for negative bias on the Au/Cr contact of the Au/Cr-Al_{0.5}Ga_{0.5}As:Cr-GaAs MIS capacitor. Neutral density filters are used to attenuate the 8000 Å light which was used to illuminate the sample.

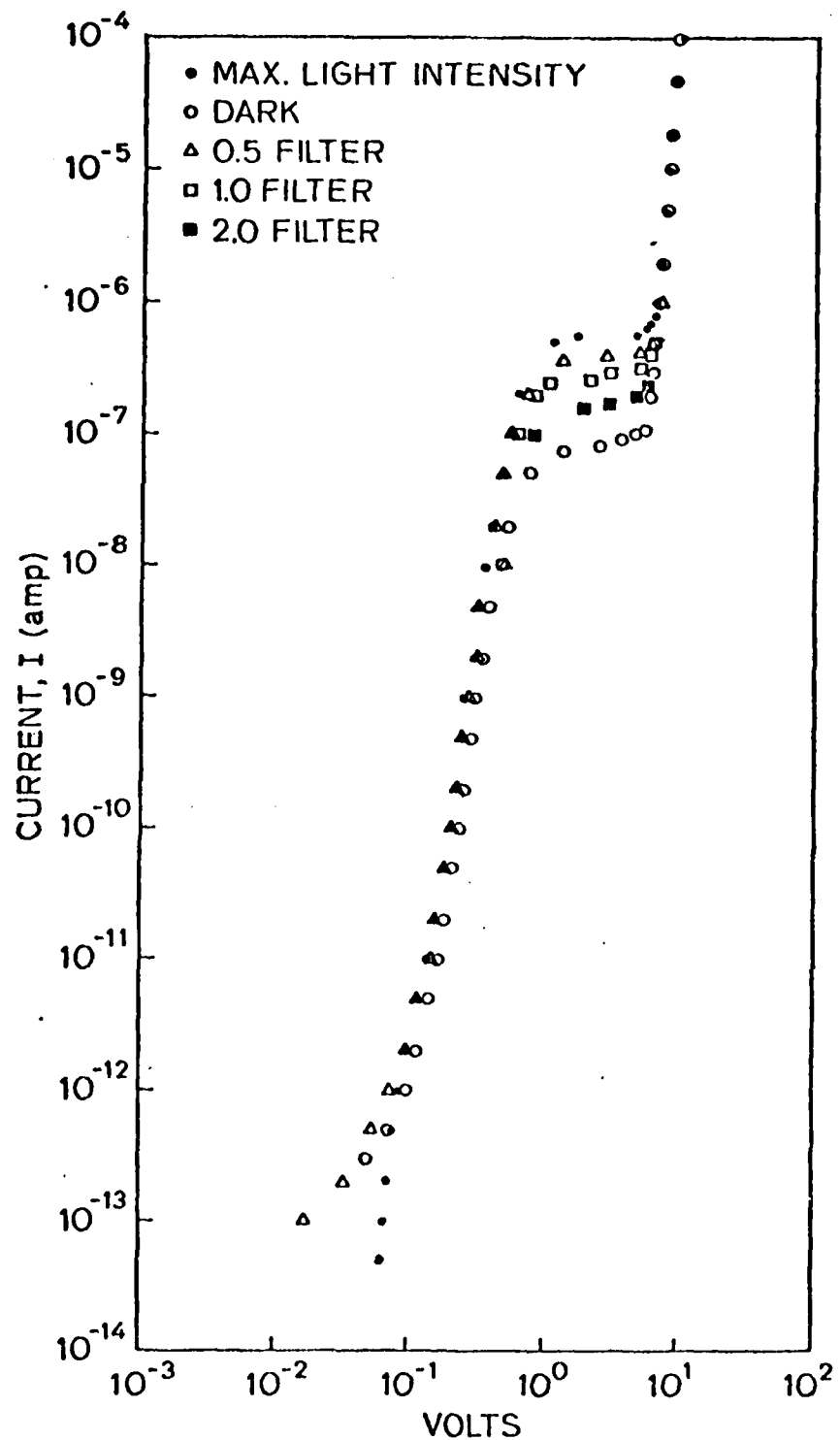


Fig. 3 Current-voltage behavior for positive bias on the Au/Cr contact of the Au/Cr-Al_{0.5}Ga_{0.5}As:Cr-GaAs MIS capacitor. Neutral density filters are used to attenuate the 8000 Å light which was used to illuminate the sample.

APPENDIX F

PREPARATION AND PROPERTIES OF $\text{Al}_x\text{Ga}_{1-x}\text{As}:\text{Cr}$
SINGLE CRYSTALS

January 1980

Quarterly Report
Covering the Period 1 October 1979
through 31 December 1979

Prepared under
Office of Naval Research
Contract No. N00014-78-C-0297

Solid-State Electronics Laboratory
Stanford Electronics Laboratories
Stanford University Stanford, CA 94305

FOREWORD

This is the eighth quarterly report on Stanford Project J-528, "Preparation and Properties of $Al_xGa_{1-x}As:Cr$ Single Crystals". The research was conducted at the Solid-State Electronics Laboratories by the following personnel:

Professor Gerald L. Pearson: Principal Investigator

Maurice Landstrass: Staff

I. Objective

The objective of this research program is to prepare semi-insulating $\text{Al}_x\text{Ga}_{1-x}\text{As}:\text{Cr}$ epi-layers for use in studying the interface properties of $\text{Al}_x\text{Ga}_{1-x}\text{As}:\text{Cr}-\text{GaAs}$ heterojunctions and to determine the utility of this system for MISFET applications.

II. Device Preparation and Electrical Measurements

The MIS diodes were fabricated from wafers consisting of an 8000Å thick $\text{Al}_{0.5}\text{Ga}_{0.5}\text{As}:\text{Cr}$ layer grown on top of a 4 micron thick GaAs layer. The latter had a nominal electron density of $1 \times 10^{16}/\text{cc}$. This heterojunction structure was grown top of a 450 micron thick (n^+) $\text{GaAs}:\text{Te}$ substrate. Diodes were fabricated by evaporating Au-Ge-Ni on the substrate and $1 \times 10^{-3} \text{ cm}^2$ Au/Cr or Pt/Cr dots on the $\text{Al}_{0.5}\text{Ga}_{0.5}\text{As}:\text{Cr}$ layer. The underlying Cr layer was ~300Å thick and the Au (or Pt) layer was ~2000Å.

Electrical studies consisted of capacitance and A.C. conductance measurements on the MIS diodes. The frequency range of the measurements extended from 10 Hz to 1 MHz. The temperature range was from 77° to 600°K. The measurements at a frequency of 1 MHz used a Boonton 72B capacitance meter while those in the frequency range of 100 kHz to 10 Hz used a lock-in technique employing a PAR lock-in amplifier and a PAR current amplifier. In all measurements the gate voltage was swept at 0.2 V/sec and the capacitance (or conductance) was recorded on an x-y recorder.

An admittance spectroscopy technique described by H. C. Casey, et al., J. Vac. Sci. Technol. 15, 1408 (1978), was employed in an attempt to determine the spatial location and energy of localized centers in the $\text{Al}_{0.5}\text{Ga}_{0.5}\text{As}:\text{Cr}$ layer. In this technique the A.C. conductance is recorded as a function of temperature with the frequency of measurement as the independent variable.

In the simple theory each such trace should yield a peak at some temperature and no signal for higher or lower temperatures.

The results of this latter technique were obscured by an exponentially rising leakage current which made determination of the peak position difficult for the bias range under study (-5 to -3 V). In this range, the leakage conductance and the D.C. I-V characteristic had an activation energy of 0.285 eV.

Figure 1 is a reproduction of recorder traces showing the variation of capacitance versus voltage at 1 MHz, 100 kHz, 10 kHz, and 1 kHz on a given device. Figure 2 shows the I-V characteristics of this same device. The I-V characteristics were discussed in detail in the last quarterly report. Figure 3 compares A.C. conductance and capacitance versus voltage of this same device measured at a frequency of 1 kHz. All measurements reported here were performed on devices held in darkness and at a pressure of 1 micron.

The dominant features of Fig. 1 are the two sharp peaks that grow with decreasing frequency which are located at -4 and +1 volt, respectively. Both of these peaks also appear in the G-V trace at the same bias voltages as evident in Fig. 3. Both peaks occur near the onset of the constant current step which appears in the D.C. characteristics. It can be seen from the figures that the peak at +1 volt occurs only when the gate voltage is swept from positive to negative voltages. This peak is relatively temperature insensitive, and a fit to an activation energy appears to yield ≈ 0.01 eV. This weak temperature dependence suggests that the frequency dispersion at this bias is due to tunnel injection of charge into states in the Al_{0.5}Ga_{0.5}As:Cr layer. This hypothesis is supported by the fact that beginning at 1 kHz and for over frequencies this peak splits into a very sharply defined doublet which is characteristic of tunneling into localized

states. The peak at -4 volts is dominated by an activation process having an energy of 0.285 eV. The role of this activated process in increasing the magnitude of the capacitance is not known at present.

Figure 4 shows traces of the 1 MHz C-V characteristic of two different devices with slightly different compensation ratios in their $\text{Al}_{0.5}\text{Ga}_{0.5}\text{As:Cr}$ layers. Since all carriers due to uncompensated donors or acceptors are swept out of the $\text{Al}_{0.5}\text{Ga}_{0.5}\text{As:Cr}$ layer, the net effect is to vary the levels of ionized donors or acceptors which in turn cause a voltage shift of the point of maximum capacitance. This difference is evident in Fig. 4. The other difference between the two traces is the magnitude of the variation of the capacitance with voltage. This difference is due to the relative response of states in the $\text{Al}_{0.5}\text{Ga}_{0.5}\text{As:Cr}$ layer to the measurement signal.

Work during the next quarter will focus on determining the relationship between the compensation ratio of the $\text{Al}_{0.5}\text{Ga}_{0.5}\text{As:Cr}$ layers and the A.C. electrical characteristics.

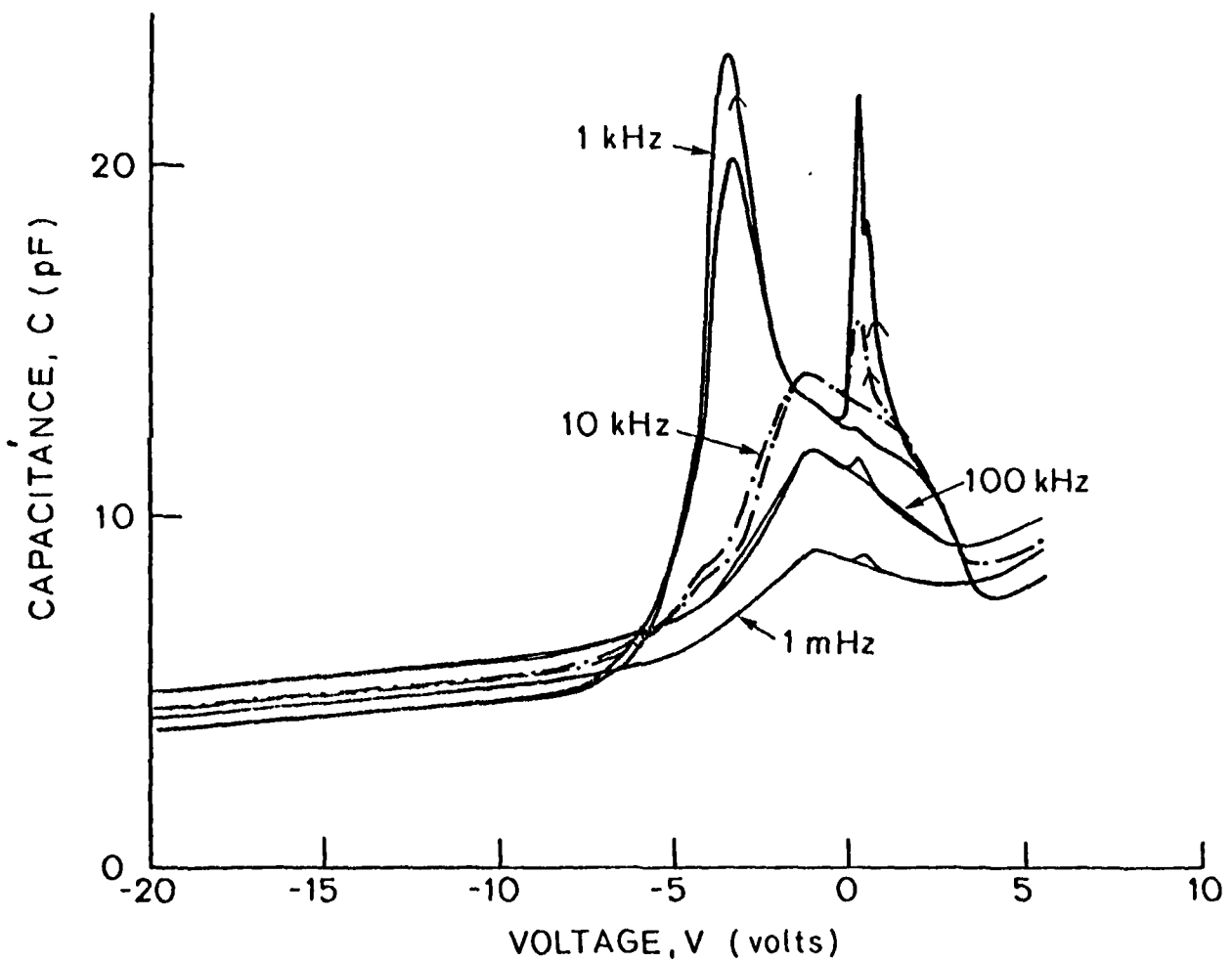


Fig. 1 Reproduction of recorder traces showing the variation of capacitance versus voltage at 1 MHz, 100 kHz, 10 kHz and 1 kHz. The device is an $\text{Au/Cr-Al}_{0.5}\text{Ga}_{0.5}\text{As:Cr-GaAs}$ MIS diode of $1 \times 10^{-3} \text{ cm}^2$ area. Measurements were performed in darkness at 1 micron pressure. The voltage refers to the polarity of the Au/Cr dot. The bias voltage was swept by a triangular waveform at a rate of 0.2V/sec.

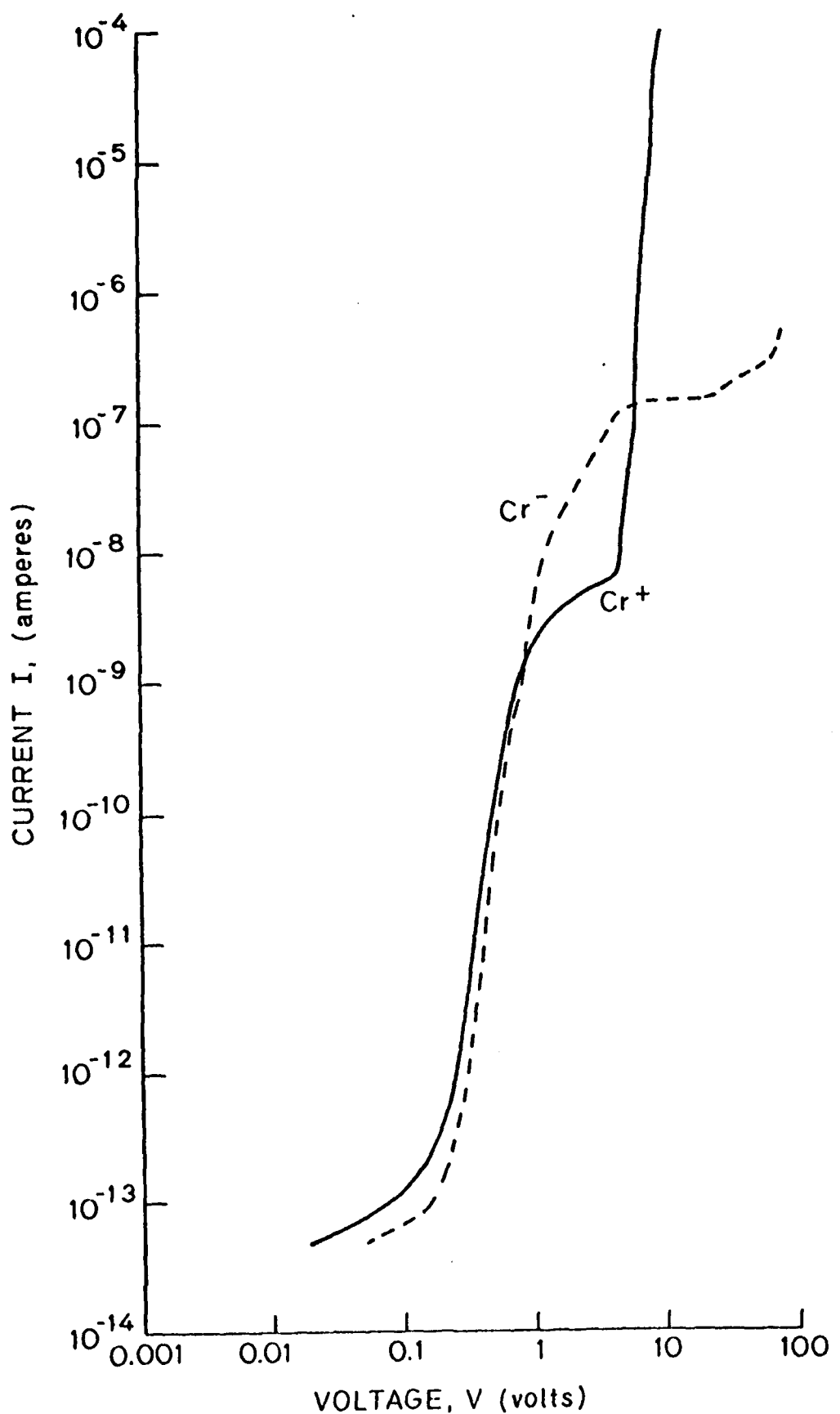


Fig. 2 Direct current I-V characteristics of the MIS diodes whose C-V characteristics appear in Fig. 1.

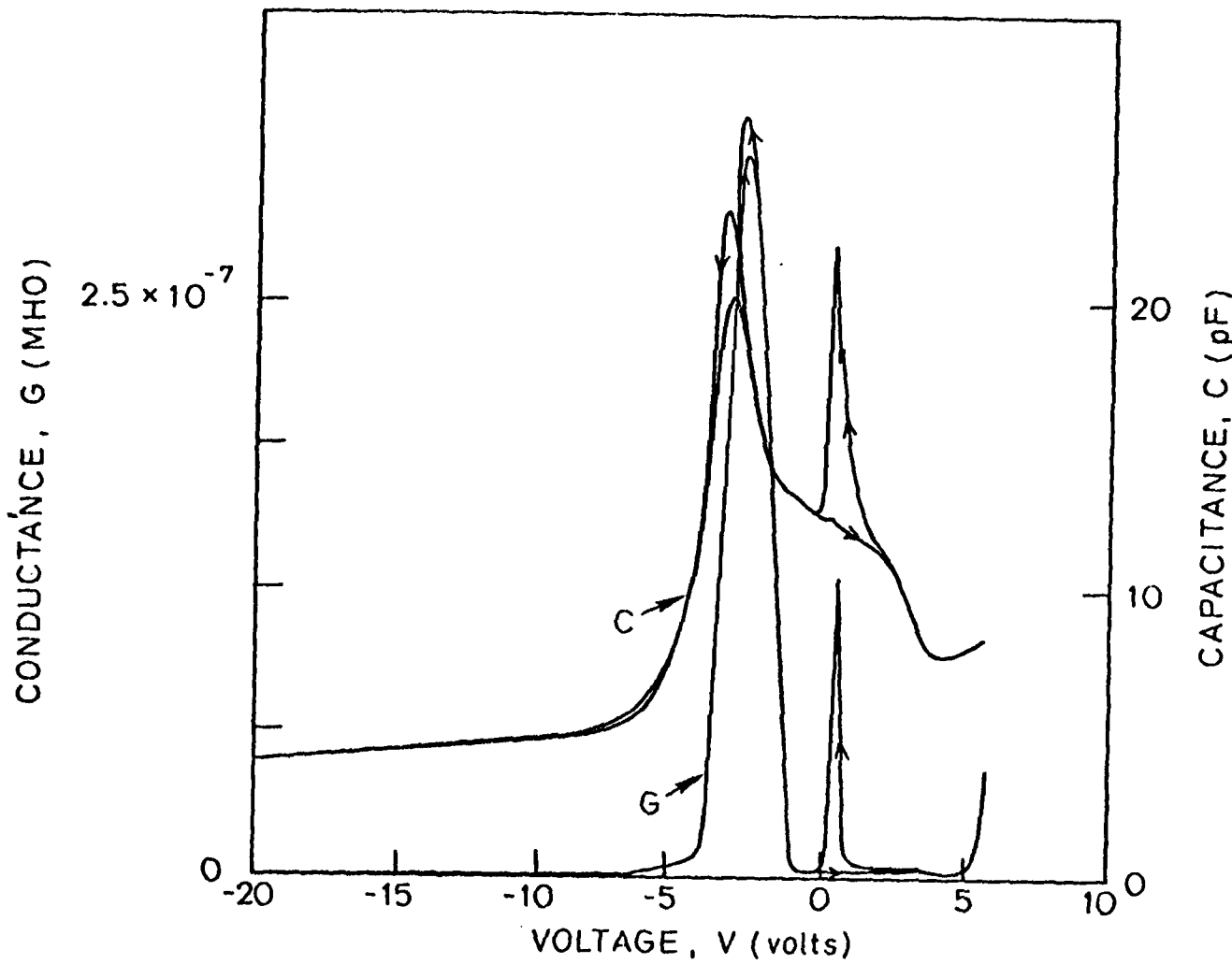


Fig. 3 Capacitance and AC conductance versus voltage for a measurement frequency of 1 kHz. The device is the same as that used in Figs. 1 and 2. The bias voltage was swept through an entire cycle of the triangular waveform used to bias the sample. The arrows indicate the sweep direction.

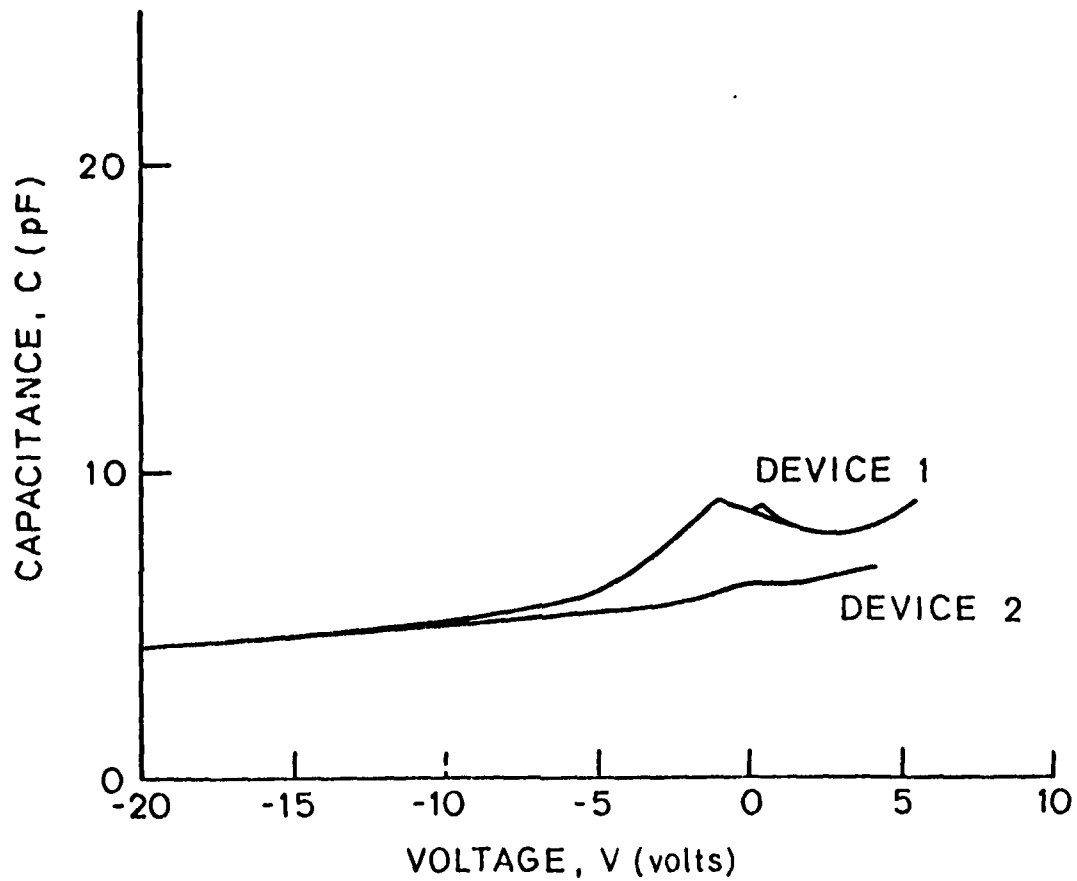


Fig. 4 Recorder traces of the 1 MHz C-V characteristics of two different devices with slightly different compensation ratios in the $\text{Al}_{0.5}\text{Ga}_{0.5}\text{As:Cr}$ layer. Device 1 is the same as that whose measurements appear in Figs. 1, 2 and 3. The two devices are identical in all other respects.

APPENDIX G

PREPARATION AND PROPERTIES OF $\text{Al}_x\text{Ga}_{1-x}\text{As:Cr}$
SINGLE CRYSTALS

June 1980

Quarterly Report
Covering the Period 1 April 1980
through 30 June 1980

Prepared under
Office of Naval Research
Contract No. N00014-78-C-0297

Solid-State Electronics Laboratory
Stanford Electronics Laboratories
Stanford University Stanford, CA 94305

FOREWORD

This is the tenth quarterly report on Stanford Project J-528, "Preparation and Properties of $Al_xGa_{1-x}As:Cr$ Single Crystals". The research was conducted at the Solid-State Electronics Laboratories by the following personnel:

Professor Gerald L. Pearson: Principal Investigator

Maurice Landstrass: Staff

I. Objective

The objective of this research program is to prepare semi-insulating $\text{Al}_x\text{Ga}_{1-x}\text{As}:\text{Cr}$ epi-layers for use in studying the interface properties of $\text{Al}_x\text{Ga}_{1-x}\text{As}:\text{Cr}-\text{GaAs}$ heterojunctions and to determine the utility of this system for MISFET applications.

II. Crystal Growth

Work during this quarter centered on the examination of impurity incorporation into the $\text{Al}_x\text{Ga}_{1-x}\text{As}:\text{Cr}$ layer from sources other than growth system reactions.

The growth parameters studied include the melt bakeout temperature, the melt bakeout time, the growth temperature, the saturation time before growth of the $\text{Al}_x\text{Ga}_{1-x}\text{As}:\text{Cr}$ layer, the thickness of the underlying GaAs layer, the Cr concentration in the melt and the impurity content of the GaAs melt.

It was found that if the melt bakeout temperature fluctuated beyond $\pm 5^\circ\text{C}$ the impurities added from the growth system reactions were the dominant variable in controlling the compensation ratio. The next most important mechanism affecting the compensation ratio was found to be contamination of the $\text{Al}_x\text{Ga}_{1-x}\text{As}:\text{Cr}$ melt by the GaAs buffer layer. The impurity content of the GaAs melt was established by the following distinct mechanisms: (1) the melt bakeout conditions, (2) contamination from the substrate, and (3) by intentionally added impurities.

It was found that GaAs layers grown from undoped melts were n-type with carrier concentrations of $\sim 5 \times 10^{16} \text{ cm}^{-3}$ when grown on (n+)GaAs:Te substrates and $\sim 5 \times 10^{15} \text{ cm}^{-3}$ when grown on SI GaAs:Cr substrates. Undoped GaAs layers which had been grown on SI GaAs:Cr substrates had no observable effect on contaminating the $\text{Al}_x\text{Ga}_{1-x}\text{As}:\text{Cr}$ layer. GaAs layers grown on GaAs:Cr substrates

that had been doped p-type with Ge to $1 \times 10^{16}/\text{cm}^{-3}$ contaminated the $\text{Al}_x\text{Ga}_{1-x}\text{As:Cr}$ layer so as to shift the compensation ratio towards p-type doping. Experiments are in progress to ascertain if this can be compensated for in a reproducible manner.

A boron doping study is underway to determine its utility in facilitating the growth of compensated $\text{Al}_x\text{Ga}_{1-x}\text{As:Cr}$ crystals. It has been reported that bulk GaAs crystals grown in the presence of B_2O_3 cannot be electrically doped with Si. Silicon is one of the major growth system contaminants in the LPE process. If this Si contamination can be easily made electrically inactive then close compensation should be facilitated. The only results to date are that melts containing up to 5 atomic percent B have no deleterious effects on the surface morphology of the grown layers.

III. Electrical Measurements on MIS Capacitors

Planar MIS capacitors were fabricated from wafers which consisted of an 8000 Å $\text{Al}_{0.5}\text{Ga}_{0.5}\text{As:Cr}$ surface layer, a 10 μm (n)GaAs ($n = 5 \times 10^{15} \text{ cm}^{-3}$) active layer and a SI GaAs:Cr substrate. The contact to the $\text{Al}_{0.5}\text{Ga}_{0.5}\text{As:Cr}$ layer was a $1 \times 10^{-3} \text{ cm}^2$ area Pt/Cr dot, and the contact to the (n)GaAs layer was evaporated and alloyed Au-Ge. I-V and C-V measurements were made at room temperature and 90K. The C-V measurements were made at selected frequencies between 10 Hz and 1 MHz.

The most interesting feature of the I-V characteristics was the magnitude of the current when the Pt/Cr electrode was made negative. At room temperature this current exceeded $1 \times 10^{-14} \text{ A}$ ($1 \times 10^{-11} \text{ A/cm}^2$) only at bias voltages greater than 12 V. At 90K this value of current was exceeded only above 20 V. Above this voltage the current rose steeply and exhibited the characteristic of tunnel breakdown. The detection limit of the electrometer used to measure the I-V characteristics is 10^{-14} A .

Figure 1 is a reproduction of the room temperature C-V characteristics taken at 100 Hz and 1 MHz whereas Fig. 2 exhibits C-V traces at 90K when taken at 100 Hz and 100 kHz.

The most distinctive feature in both figures is the large frequency dispersion at zero bias. This is attributed to charge injection and trapping in the $\text{Al}_{0.5}\text{Ga}_{0.5}\text{As:Cr}$ layer. This is also the cause for the large change in the high frequency traces with temperature. The other notable feature of the C-V traces is the saturation of the capacitance at negative biases. This occurs at a voltage where the Fermi level in the GaAs layer crosses into the valence band. The 100 Hz characteristics show no modulation due to inversion charge that would be expected for this configuration. At this bias the leakage current is too small to measure. This result indicates that, although the leakage current is too small to push the device into deep depletion, any excess holes must leak away from the interface. The point at which the capacitance saturates varies with temperature and is characteristic of the temperature variation of the electron density in the GaAs layer.

IV. Interface Transport Measurements

The major problem with MIS devices on GaAs which use deposited insulators or native oxide insulators is that the interface state density at the GaAs interface is large. This prevents the operation of such devices in the inversion mode due to their insensitivity to dc bias. To date, every attempt to measure interface state density at the $\text{Al}_x\text{Ga}_{1-x}\text{As-GaAs}$ interface has been unsuccessful and the reason most often mentioned has been lack of sensitivity to detect the small number of states believed to be present.

The heteroepitaxial insulator SI $\text{Al}_x\text{Ga}_{1-x}\text{As:Cr}$ has a different physical mechanism than those above that most likely inhibits inversion behavior to

be exhibited in such MIS capacitors. This is the conduction of inversion charge away from the heterojunction interface. In Si the generation rate is $\sim 10^4$ higher than in GaAs. From published results, a typical SiO_2 -Si interface loses its inversion charge at the interface when gate leakage currents are above $\sim 10^{-9} \text{ A/cm}^2$. This implies that, at the insulator-GaAs interface, a leakage current in excess of 10^{-13} A/cm^2 is sufficient to remove any thermally generated inversion charge.

In a device, generation rate is not important since inversion charge is supplied by injection from the source/drain contacts. The first order materials property of an MIS device is the reduction in interface states and not the reduction of leakage current.

A structure was designed during this quarter to study the transport properties of injected minority charge at the heterojunction interface. The structure has a Pt/Ni gate, designed to modulate the GaAs surface potential by means of an applied gate voltage. The main feature of this device is that the gate and source/drain contacts are self aligned so that no critical masking steps are involved. Starting with a grown wafer as described in Section III, the device is fabricated as follows. First the wafer is diced into $2 \times 1 \text{ mm}$ chips. Then $1 \mu\text{m}$ of Ni is evaporated onto the top surface. A small Pt dot is then evaporated in the middle of the Ni layer. The entire structure is next heated in O_2 for 0.5 hour at 630°C to oxidize the outer surface of the Ni layer (except under the Pt dot) as well as the edge regions of the AlGaAs layer. Then Au/Zn is deposited on the sides of the chip to form the source and drain contacts after which the structure is heated in H_2 to diffuse Zn into the GaAs and GaAs:Cr layers. Figure 3 is a cross section diagram of the completed device. The critical feature of this process is that the oxidation step provides insulation between the gate and the

source/drain contacts without masking, and also provides a barrier so that Zn does not diffuse through the AlGaAs layer.

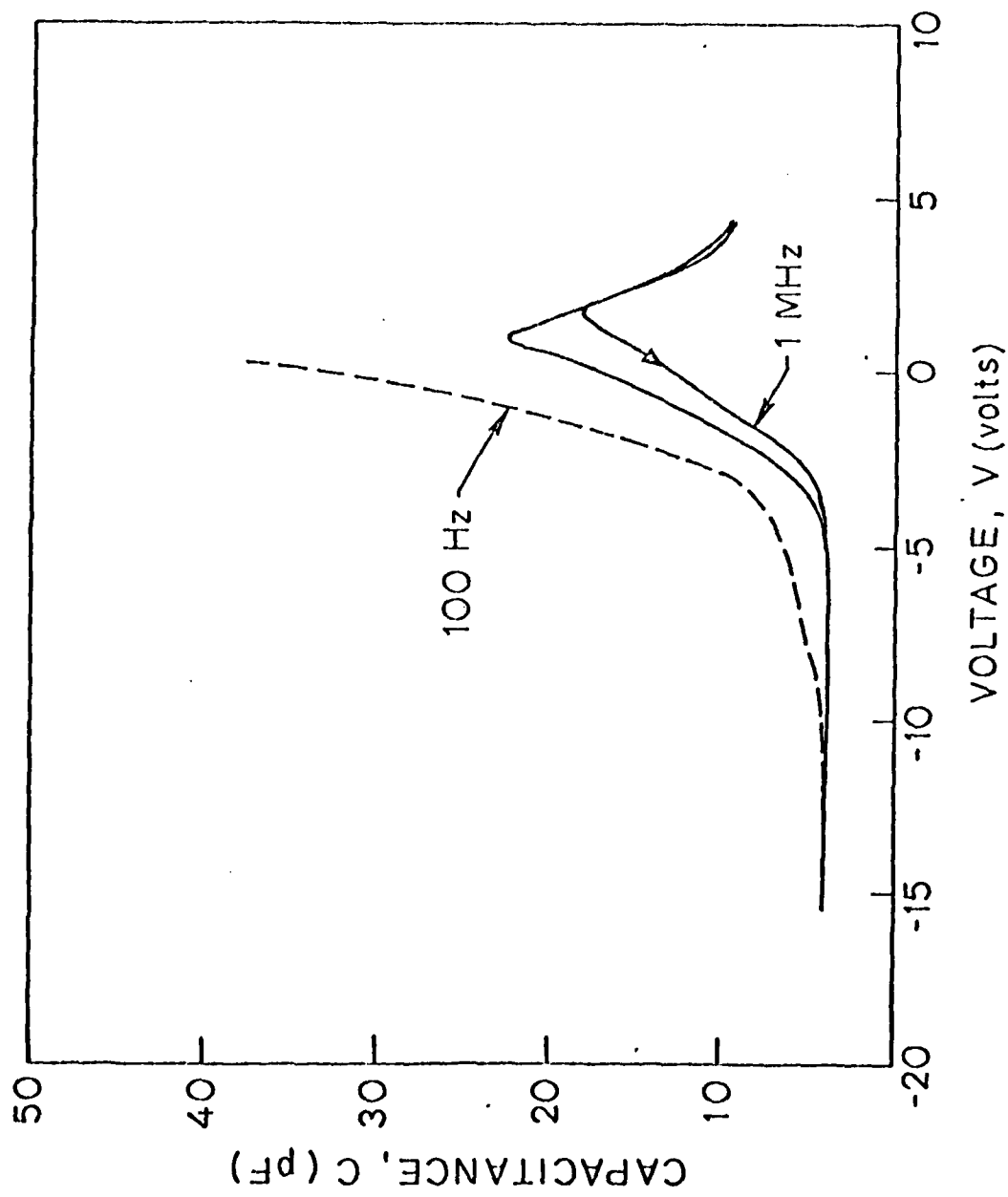


Fig. 1 C-V characteristics of a planar MIS capacitor measured at 100 Hz and 1 MHz. The capacitor area is $1 \times 10^{-3} \text{ cm}^2$. The measurements were made at room temperature in darkness and at 10^{-3} Torr. The gate voltage was swept at 0.2 V/sec. Measurements were made with a lock-in technique.

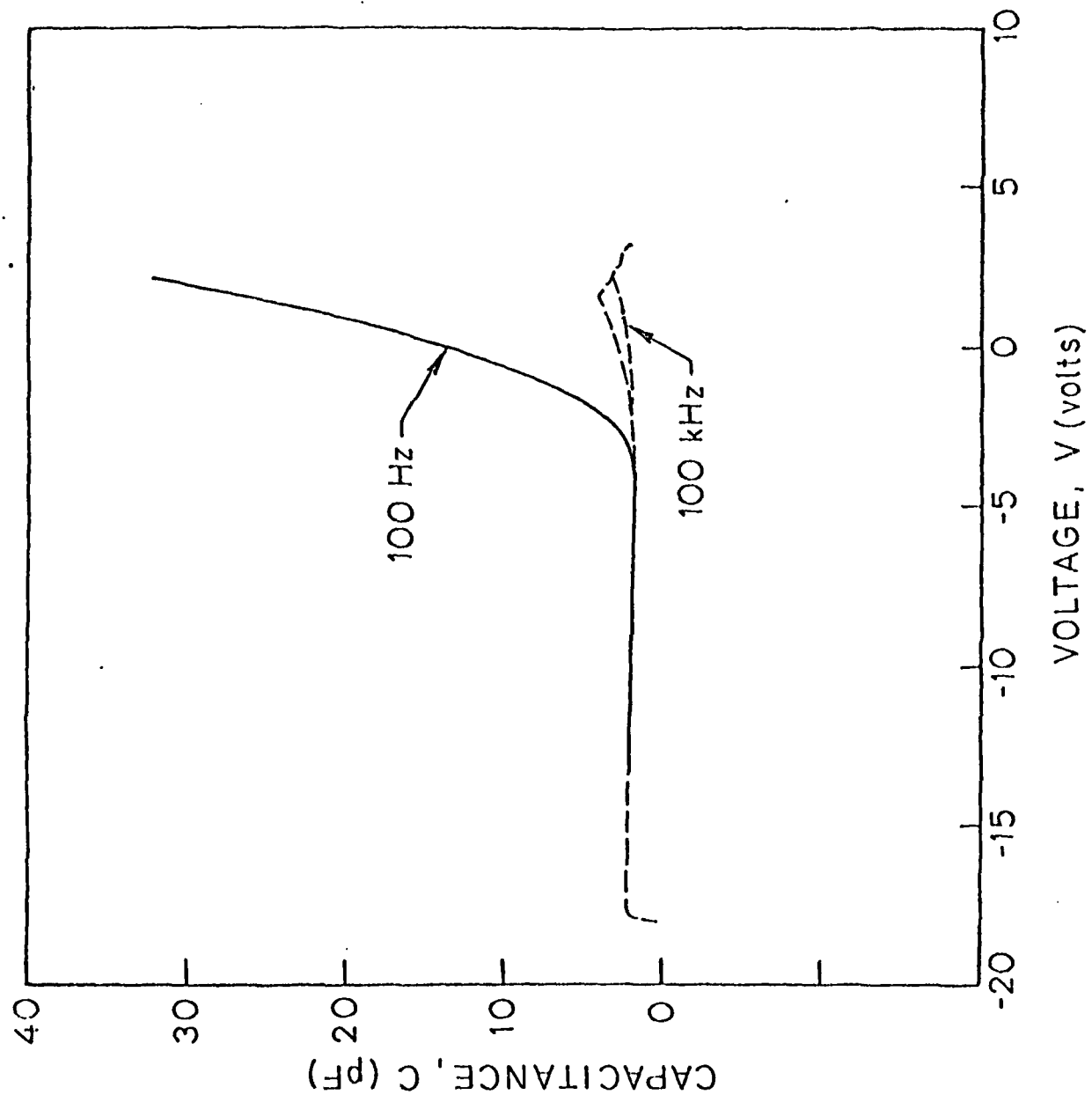


Fig. 2 C-V characteristics measured at 90K. The measurement frequencies were 100 Hz and 100 kHz. All other conditions are the same as in Fig. 1.

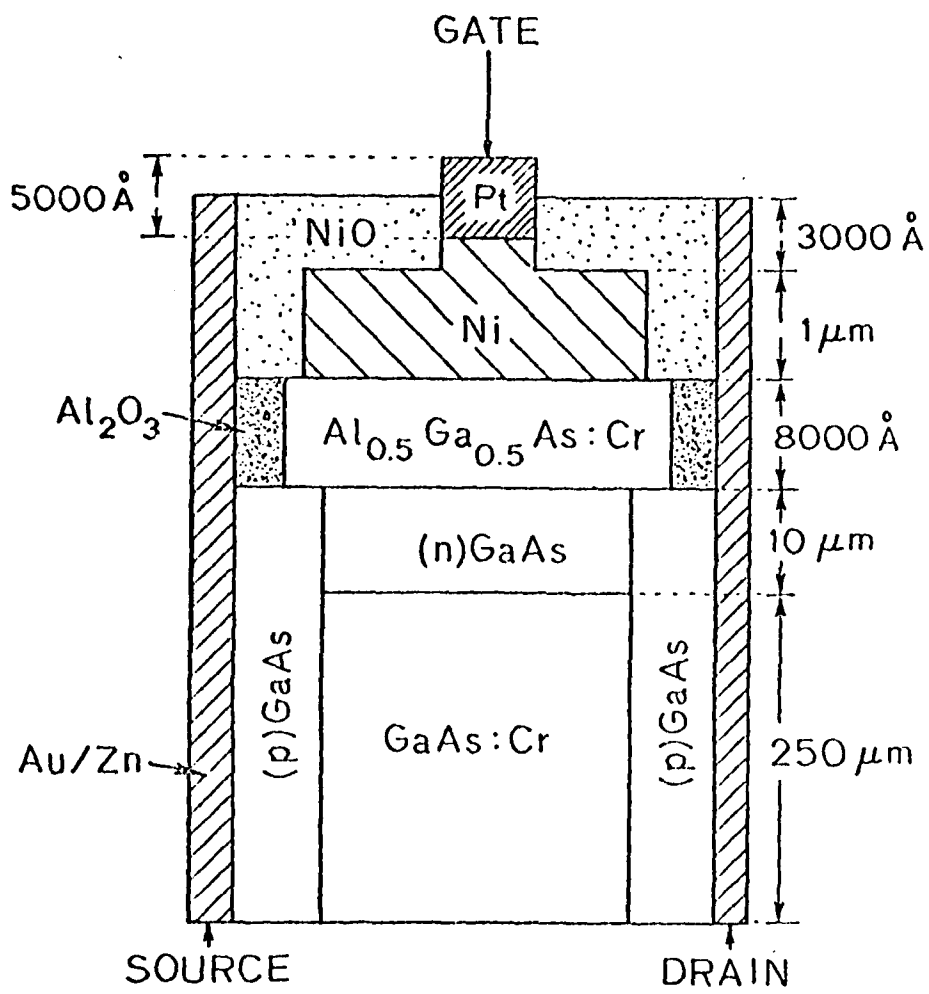


Fig. 3 Schematic diagram of self-aligned MIS inversion mode transistor. Device pictured is for transport measurements of a hole inversion layer. Holes are supplied by p-type injecting source/drain contacts.

Distribution List

Dr. Howard Lessoff
Code 5220
Naval Research Laboratory
4555 Overlook Avenue, S.W.
Washington, DC 20375

Dr. Harry Wieder, Code 746
Electronic Materials Sciences Division
Naval Ocean Systems Center
San Diego, CA 92152

Mr. Elmer Keith
ONR Resident Representative
Durand Aeronautics Bldg., Room 165
Stanford, CA 94305

Scientific Officer
ONR Branch Office
1030 East Green Street
Pasadena, CA 91106

NRL (6 copies)
Code 2627
Naval Research Laboratory
Washington, DC 20375

DDC (12 copies)
Defense Documentation Center
Bldg. 5, Cameron Station
Alexandria, VA 22314